Performance of the CORDEX-Africa Regional Climate Model in capturing precipitation and air temperature conditions in the Omo Gibe River Basin, Ethiopia

Yonas Mathewos (yonasmathewos4@gmail.com)
Faculty of Biosystems and Water Resources Engineering, Institute of Technology, Hawassa University
Brook Abate
College of Architecture and Civil Engineering, Addis Ababa Science and Technology University
Mulugeta Dadi
Faculty of Biosystems and Water Resources Engineering, Institute of Technology, Hawassa University

Research Article

Keywords: Climate conditions, CORDEX-Africa, Multi-model ensemble, Performance, RCM

Posted Date: December 14th, 2022

DOI: https://doi.org/10.21203/rs.3.rs-2358014/v1

Abstract

Using regional climate models (RCMs) and ensembles of multiple model simulation outputs without assessing their modeling performance did not always ensure the best agreement between observed and modeled climate variables. To this end, assessing the modeling performance of regional climate models (RCMs) is indispensable in selecting the most effective model to use for climate change impact studies. In this study, the performance of ten Coordinated Regional Climate Downscaling Experiments (CORDEX) in Africa was examined against observational datasets from 1986 to 2005 across the entire Omo Gibe River Basin (OGRB). The output of RCMs was evaluated based on their ability to reproduce the magnitude and pattern of monthly, seasonal, and annual precipitation and air temperature, precipitation characteristics, and statistical metrics. The results confirm the difference between RCMs in capturing climate conditions at both spatial and temporal scales. The spatial pattern of mean annual precipitation was better reproduced by the ensemble mean and RACMO22T (EC-EARTH). CCLM4-8-17 (MPI) and the ensemble mean reproduced the annual patterns of observed precipitation, even though the amounts were different. Except for peak precipitation, all RCMs simulated seasonal precipitation, and the pattern was reasonably captured by RACMO22T (EC-EARTH), CCLM4-8-17 (CNRM), RCA4 (CNRM), CCLM4-8-17 (MPI), and REMO2009 (MPI). The interannual and seasonal variability of precipitation was higher than the variability of air temperature. It was found that observed and RCM precipitation simulations using CCLM4-8-17 (MPI), REMO2009 (MPI), and RCA4 (CNRM) showed better agreement at several individual stations in the Omo Gibe River Basin (OGRB. Likewise, RCA4 (MPI) and CCLM4-8-17 (MPI) were superior in capturing minimum and maximum air temperatures. The cumulative distribution of extreme precipitation was better captured by RCA4 (MIROC5), and all RCMs, including their ensemble mean, overestimated the return period. Overall, the study emphasizes that the selection of robust RCMs that better reproduce observed climate conditions and the use of multi-model ensembles of models with the best performance after systematic bias correction are fundamentally necessary for any study of climate change impacts and adaptation in the OGRB.

1. Introduction

The effects of climate change are a reality everywhere in the world, regardless of their cause, and its threats are much more severe in developing and poor countries (Asfaw et al., 2021; Demissie & Sime, 2021; Dibaba et al., 2019; Ofoegbu et al., 2019). In these regions, recovery from climate change risks is made difficult by their poor adaptability, excessive dependence on ecosystem resources for their livelihood and conventional agricultural systems (Asfaw et al., 2021; Demissie & Sime, 2021; Dibaba et al., 2019; Ofoegbu et al., 2019; Warnatzsch & Reay, 2019). Moreover, the multifaceted connection between the climate system and numerous natural earth processes, such as the hydrological cycle, biodiversity, and ecosystem health, outspreads the potential impacts of climate change on the subsistence of multiple human activities in very different ways.

Africa's CO_2 emissions are much lower than the rest of the world, but the continent is one of the most vulnerable regions to the effects of climate change, particularly susceptible in sub-Saharan regions (Adenuga et al., 2021). Climate change has increased temperatures across the continent, and in some cases caused prolonged heat waves (Mueller & Seneviratne, 2013). Along with rising temperatures and frequent fluctuations in rainfall in the region, existing challenges in agricultural production, food security, health, poverty, water resources, energy, and ecosystem services are expected to worsen (Ayugi et al., 2021; Demissie & Sime, 2021; Francisco & Camargo, 2020; Warnatzsch & Reay, 2019). Moreover, agricultural expansion, rapid population growth, and increased demand for freshwater resources, coupled with the horrible consequences of excessive hydrological events, including floods and prolonged drought have worsened conditions in the region (Ayugi et al., 2021; Demissie & Sime, 2021).

In Ethiopia, agriculture is the spine of the financial system, and the source of food for the majority of the population (Yigezu, 2021; Welteji, 2018). About 90% of agricultural productivity relies on rainfall, and its variability in tandem with air temperature has induced a significant impact on the sector (Asseng et al., 2015). The main reason for the country's extreme vulnerability to climate variability and change is due to heavy dependence on rain-fed agriculture, underdevelopment of water resources, and poor river basin management practices (Anose et al., 2022; Gebrechorkos et al., 2019; Moges, 2013). The country is regularly subject to famine and various socioeconomic disasters (Anose et al., 2022; Teshome & Zhang, 2019). Therefore, the effects of climate change are a serious challenge regarding the sustainability of water resources and agricultural production in the country of Ethiopia.

Accurate information on regional climate models (RCMs) is needed to fill the gaps due to the lack of country-specific instruments for assessing regional and local effects of climate change, conducting impact assessments, and developing adaptation strategies at the regional or national level (Demissie & Sime, 2021; Guo et al., 2018). Examining how historical climate has recorded observational data plays a major role in better estimating future climate change and assessing its impacts from multiple perspectives (Pang et al., 2021). Since its invention, the Global Climate Model (GCM) output has been used in several studies to predict future changes in the earth's climate (Ayugi et al., 2021; Girma et al., 2022). Various scholars have described the coarse spatial resolution of GCMs as having limitations in projecting climate change at a local scale (Demissie & Sime, 2021; Dibaba et al., 2019; Stefanidis et al., 2020). The coarse resolution also prevents global models from accurately describing extreme hydrological events (Girma et al., 2022; Worku et al., 2018). Therefore, to obtain appropriate temporal and spatial scales for local climate change impact studies, it is essential to downscale climate model output from low spatial resolution GCMs to the highest regional scale resolution.

Currently, different organizations use the results of RCM simulations to conduct local detailed studies of climate impacts and to explain land surface heterogeneity (Ayugi et al., 2021; Dhidiou et al., 2014). The Coordinated Regional Climate Downscaling Experiment (CORDEX) provides local-scale information for the climate modeling community and relevant climate information for end users (Gutowski et al., 2016). CORDEX-Africa is an initiative launched by the World Climate Research Program (WCRP) to downscale various GCM outputs and produce an ensemble of high-resolution (~ 50 km) historical and future climate projections for the African continent (Dibaba et al., 2019; Worku et al., 2018). RCM simulations are useful for understanding local climates in regions with complex topography (Warnatzsch & Reay, 2019). Moreover, RCMs act as a zooming device to provide climate information at regional and local scales (Akinsanola et al., 2015; Ayugi et al., 2021). Several studies have shown that RCMs reproduce the most reliable annual and seasonal estimates of precipitation and air temperature, and are preferred in analyzing the distribution and frequency of extreme precipitation (Dosio et al., 2015; Worku et al., 2018). A study by Warnatzsch & Reay, (2019) reported that RCMs performed well in simulating air temperature, which resulted in the poor simulation of precipitation, so their

performance was variable. Luhunga et al., (2016) used observed station data to evaluate CORDEX-RCMs in reproducing climate variables and found that RCMs perform differently over a wide region of Tanzania. In addition, Mutayoba & Kashaigili, (2017) for Africa showed that the ensemble matched the observed data better than the individual RCMs. In Ethiopia, some studies have shown that RCMs are biased at high altitudes but perform well in lower-altitude regions (Demissie & Sime, 2021; Dibaba et al., 2019; Van Vooren et al., 2019; Worku et al., 2018). In the country, research has focused on climate change vulnerability and mitigation measures using single RCM simulations (Endris et al., 2016; Etana et al., 2021). According to Dibaba et al., (2019); Mutayoba & Kashaigili, (2017), not all RCMs are equally important in terms of their effectiveness in capturing a localized study area. The inconsistency in the performance of RCMs when capturing in different regions and seasons implies an evaluation of the sensitivity of a region using several available RCMs and is necessary to select the most effective RCMs for specific regions.

This study aimed to assess how well the Coordinated Regional Climate Downscaling Experiment (CORDEX) RCMs in the African domains reproduce the climate conditions in the Omo-Gibe River basin (OGRB), Ethiopia. Ten RCMs that have been widely used in local-scale climate change impact studies across Africa, particularly in East Africa were evaluated. RCMs simulation outputs were evaluated based on statistical metrics, annual and seasonal temperature, and precipitation from actual ground observation data. In addition, a spatial distribution of precipitation for the entire basin was developed, taking into account the cumulative distribution of the areal extreme precipitation, and the frequency of extreme precipitation was analyzed. Analysis and comparison of individual RCMs and their ensembles will help us to better understand at the local scale how RCMs behave in areas of complex topography in capturing the climatology of the OGRB in Ethiopia.

2. Materials And Methods

2.1 Description of the study area

This study was conducted to cover the entire Omo Gibe River Basin having an area of about 79000 km^2, and is situated southwest of Ethiopia.

2.2 Regional and Global Climate Models (RCMs and GCMs) data

The RCMs simulated precipitation and air temperatures on a temporal resolution of the daily time step for the period 1986–2005 obtained from the Coordinated Regional Climate Downscaling Experiment Program (CORDEX) fed by six CMIP5 GCMs. Historical GCM simulations used as initial boundary conditions were initialized with atmospheric, ocean, land, and sea surface temperature (SST) conditions and constrained by observed natural and anthropogenic concentrations of CO_2 and aerosols (Taylor et al., 2012; Worku et al., 2018). For each RCM, the historical simulation and only the first ensemble member (r1) were considered. The results of these simulations were obtained from the CORDEX project in the African domain with a spatial resolution of nearly 0.44° * 0.44°. The selected RCMs in CORDEX Africa domains included CanRCM4, RACMO22T, REMO2009, RCA4, and CCLM4-8-17 and the details of the RCMs used to regionalize the GCMs are listed in Table 1 along with their characteristics. The simulated historical period is available from 1950 to 2005; however, common periods from 1986 to 2005 are used for all RCMs. These models have been evaluated in several studies on Africa and found to be effective in simulating rainfall and air temperature (Demissie & Sime, 2021; Dibaba et al., 2019; Dosio et al., 2015; Worku et al., 2018). In the Omo Gibe River Basin, the performance of the CORDEX Africa domains has not previously been evaluated using different RCMs, except in studies conducted by Demissie & Sime, (2021) in the Jimma area, upper Gilgel Gibe districts. The RCM precipitation and air temperature data were downloaded from a public website of the Earth System Grid Federation (ESGF) using the link: https://esgf-node.llnl.gov/search/esgf-llnl/, the required data for each station is extracted using the station's latitude and longitude in ArcGIS.

Table 1
List and description of RCM and boundary conditions used with their simulation acronym

Description of the RCMs	Driving GCM Name	RCMs	Reference
Koninklijk Nederlands Meteorologisch Institute (KNMI), Regional atmospheric climate model version 2.2, Netherlands	ICHEC-EC-EARTH	KNMI-RACMO22T	(Meijgaard et al., 2008)
Sveriges Meteorologiska och Hydrologiska Institute (SMHI), The Rossby Centre Regional Climate model, Sweden	CNRM-CERFACS-CNRM-CM5 MPI-M-MPI-ESM-LR MOHC-HadGEM2-ES MIROC-MIROC5	SMHI-RCA4	(Samuelsson et al., 2011)
COnsortium for Small-scale MOdeling (COSMO) Climate Limited Area modelling Community (CLMcom), USA	CNRM-CERFACS-CNRM-CM5 MOHC-HadGEM2-ES MPI-M-MPI-ESM-LR	CLMcom-CCLM4-8-17	(Platonov & Kislov, 2020)
Max Planck Institute for Meteorology-Climate Service centre (MPI-CSC), Regional Model, Germany	MPI-M-MPI-ESM-LR	MPI-CSC-REMO2009	(Jacob et al., 2007)
The Canadian Centre for Climate Modeling and Analysis second generation Earth System Model, Canadian Regional Climate Model version 4	CCCma-CanESM2	CCCma-CanRCM4	(Caya et al., 1995; Zadra et al., 2008)

2.3 Observed meteorological data

In Ethiopia, the lack of meteorological observation data over long periods limits the ability to understand which processes in climate model representations are most in need of improvement. Most of the meteorological gauging networks were installed in the country after the drought in the mid-1980s. The performance evaluation of the RCM simulation result requires observed data or reference data. Even though there are large discrepancies between the actual gauge-based datasets and the satellite datasets, several scientists have used satellite data to verify the RCM results. The climatology of the real observational measurements of the ground network has been reproduced, allowing the detailed evaluation of the simulated precipitation at the regional scale (Diro et al., 2011). Therefore, daily air temperature and precipitation data from actual weather stations obtained from the National Meteorological Service Agency of Ethiopia were used for this study. The record duration of 20 years from 1986 to 2005 for twenty meteorological stations included in the descriptive map of the study area Fig. 1 was considered to adequately reflect the climatology of the basin. Usually, climate analysis requires complete data sets with no gaps and missing records, the continuity of a record can be broken with missing data due to the absence of the observer and the failed instrument. Therefore, it is necessary to estimate and complete the missing data before using it for hydrological analysis. The specific technique for integrating missing data is called data imputation. The choice of this method is based on the percentage of data lost and the choice of neighboring stations. In this regard, precipitation stations with many missing values and stations with only precipitation records are not eligible for evaluation. Consequently, the meteorological stations described in Table 1 with the precipitation and temperature records were used for the analysis in the basin. In both cases, all stations have missing values of less than 6 percent for the 1986–2005 records. Missing data were filled in before analysis using XLSTAT 2018 software. It is statistical software that has been used to examine the relationships of several variables at the same time (Vidal et al., 2020).

The quality and reliability of the observed data from all stations were examined in the homogeneity test. In this study, data homogeneity was checked using the standard normal homogeneity test (SNHT) in XLSTAT. This method was used to identify a variation in a time series of precipitation data by comparing the mean of the first k years of the record with the last n-k years (Agha et al., 2017; Demissie & Sime, 2021a; Elzeiny et al., 2019). Errors such as minimum temperature above maximum temperature and negative precipitation values were corrected using nearby stations. Outliers, such as data outside the mean of ± four times the standard deviation, were changed to mean values from the days before and after the outlier day (WMO, 2009). The homogeneity of the observed data was verified, and the data of all the stations considered were found to be homogeneous.

2.4 Methods

In general, two performance evaluation criteria were used to measure how well climate models replicate or simulate the climatology of the entire basin under study. The first criterion evaluates the ability of RCMs to reproduce the climatology of precipitation and the characteristics of rainfall events. This criterion compared the mean annual and seasonal precipitation magnitude, mean monthly precipitation pattern, distribution, frequency of precipitation events, and return period of the RCM results to that of the observed data. As a second evaluation criterion, statistical metrics were used, which are described in detail in the following section.

2.4.1 Model performance evaluation metrics

The validation of climate models to reproduce observed climate variables such as precipitation and temperature for the reference period is exceptional in terms of their potential application to the projected data set for future studies of climate change impacts in the Omo Gibe River Basin, Ethiopia. Therefore, the systematic and dynamic behavior of the models was visualized by plotting the simulated and observed data on the same coordinate system. Not all models were equally capable to simulate climate data, as they are influenced by factors such as the characteristics of the land. To evaluate the performance of RCMs in simulating average annual precipitation and air temperature, several statistical approaches are widely used. They include the mean percentage of bias (PBIAS), the Root Means Square Error (RMSE), and the Pearson correlation coefficient (r) which are commonly used, and the performance of these evaluation metrics have been explained and supported in multiple studies (Demissie & Sime, 2021; Dibaba et al., 2019; Martynov et al., 2013; Mendez et al., 2020; Ongoma et al., 2019; Yimer et al., 2022).

The absolute percentage biases between the results of the regional climate model and the observed climatology were calculated for both precipitation and temperature. The absolute percentage bias indicates the systematic error between the RCM and the actual climatology of the ground station. Negative values indicate an underestimate, while positive values indicate an overestimation of climate models. The values closest to zero show a minimum systematic difference and the best estimate of the climate models. Subsequent empirical equations were used to explain the absolute bias for precipitation and temperature of the ten selected climate models and the mean ensemble over the Omo Gibe river basin to study spatial coherence and integrity in space.

$$\mathrm{BIAS} = \frac{1}{\mathrm{n}} \sum_{\mathrm{i}=1}^{\mathrm{n}} (\mathrm{S_i} - \mathrm{O_i})(1)$$

RMSE is the absolute error of climate models when simulating climate variables and measures the difference between RCM results and actual observational climatology. RMSE has the same unit as the observed variable, making its interpretation relatively simple. An RMSE value close to zero indicates favorable performance.

$$\mathrm{RMSE} = \sqrt{\frac{1}{\mathrm{n}} \sum_{\mathrm{i}=1}^{\mathrm{n}} (\mathrm{S_i} - \mathrm{O_i})^2} (2)$$

The correlation coefficient (r) and the coefficient of determination (r^2) are among the many approaches commonly used in various studies. Pearson's correlation coefficient measures the goodness of fit and linear association between two variables for example between RCM and observed station climatology

(Bayissa et al., 2017; Diaconescu et al., 2016; Shiferaw et al., 2018). It measures how well climate indices based on the climate model reproduce or explain observed climate indices. Although the daily input data of the time series were used to calculate the values of the climate indices, the time scale of the climate indices is annual. This makes the data length relatively short for accurately estimating Pearson's correlation coefficient values over the reporting period. Instead, the pattern correlation coefficient (sometimes called map correlation) was calculated between the maps using the climatic mean values of the climatic indices from the observed data and the RCMs in the Omo gibe river basin. Pearson's correlation coefficient is used in this study and its mathematical formulation is shown below. Its value is between 1 and − 1. A positive indicates a strong positive relationship, while a negative indicates a strong negative relationship, and zero indicates a weak or no relationship.

$$r = \frac{\sum_{i=1}^{n} (S_i - S_m)(O_i - O_m)}{\sqrt{\sum_{i=1}^{n} (S_i - S_m)^2} \sqrt{\sum_{i=1}^{n} (O_i - O_m)^2}} (3)$$

Where S is the simulated value of the RCMs and O is the observed value of the climatic variable, i refers to the simulated and observed pairs, n is the total number of pairs and m refers to the mean.

In general, the smaller the absolute value of bias and the smaller the RMSE, the better the performance of the model and vice versa. The value of the correlation coefficient can vary from − 1 for a perfect negative correlation to 1 for a perfect positive correlation between the RCMs and the observed climatic variables. In many cases, there is no single criterion that reliably indicates the best RCMs. Thus BIAS, RMSE, and r are used in combination. It is possible to have an acceptable deviation of r from 1, while it is not possible to have an acceptable common value for BIAS and RMSE. In this regard, there is no acceptable limit, except that the lower the BIAS and RMSE, the higher the accuracy of the model prediction. However, too low values could also lead to over-refinement.

2.4.2 Coefficient of Variations in precipitation and air temperature

The coefficient of variation (CV) was used to analyze seasonal and annual variations in precipitation data. The higher the CV value, the more variable the data, with values below 20 indicating low variability, values between 20 and 30 indicating moderate variability, and values above 30 indicating high variability in the recorded data (Mekonen & Berlie, 2020).

$$CV = 100^* \frac{\sigma_R}{\bar{R}} (4)$$

Where the symbol with a bar indicates the average statistical operation throughout the analysis period (1986–2005); the period of analysis (N) is 20 years; R denotes the average amount of precipitation in the basin in a given year (t); σ refers to the standard deviation of the RCM or actual observed data. R without a subscript indicates that the statistics are estimated separately for RCM or gauge basin precipitation. The calculated CV for precipitation measured and simulated by the RCM assesses the extent to which the variability of precipitation is captured by the stations in the network and represented by the RCMs.

RCM simulations should capture the deviation of annual precipitation from the long-term mean to show the consistency of model simulations. Accordingly, the compared precipitation anomaly (RA) of the RCM data and the gauge data defined for the gauge data here for a given year (t) is as follows:

$$RA = \frac{R_t - \bar{R}}{\bar{\sigma}} (5)$$

The variables in the above equation have been defined previously. This equation is applied separately for gauge precipitation and RCM precipitation data.

The second evaluation criterion used in this study is to evaluate the annual cycles of precipitation and temperature. The study of how RCMs reproduce the seasons of precipitation and temperature is analyzed. Third, the ability of individual RCMs and the mean ensemble to reproduce the inter-annual variability of precipitation and temperature across the entire basins. For this study, the time series of spatially averaged precipitation and temperature anomalies from June to September (JJAS) and March to May (MAM) are analyzed.

2.4.3 Spatial analysis of the precipitation data

The quality of the RCM simulation output can be evaluated from the actual measurements of the weather station. In this regard, there are several approaches to obtaining the RCM grid climate parameters at a location of a weather station to compare them with equivalent parameters. The study by Ly et al., (2011) on the spatial interpolation of daily precipitation on regular grids of catchments showed the comparison of different geostatistical and deterministic approaches. The study found that performance varied slightly with the density of the measuring stations and varied significantly for a smaller number of stations. The study found that simple Kriging and inverse distance weighting produced the smallest RSME values and are therefore considered to be better-performing methods. Similarly, the study by Hartkamp et al., (1999) showed comparisons of interpolation methods and indicated that IDW produces a better result. In this study, by roughly comparing IDW with kriging and spline methods, it was found that ordinary kriging estimates are better when the number of stations to be used is larger. After the RCM simulations are extracted by ArcGIS 10.4 using four grid points around each observational station, the simulated values are interpolated to the observed station using ordinary kriging. In these methods, the weights of each interpolated point are calculated based on the spatial structure of the interpolated location of all sampled points. The weights are determined from the variogram according to the spatial structure of the data and applied to the sampled points, defined mathematically as follows:

$$\widehat{Z}\left(X_o\right) = \sum_{i=1}^{N} \lambda_i Z\left(X_i\right) (6)$$

Where the value of the predicted point (z-hat, at position x-naught) is equal to the sum of the value of each sampled point (x, at position i) multiplied by the unique weight of that point (lambda, for position i). The covariance matrix of the estimated variogram is used to calculate the weights (slightly different depending on the type of kriging performed).

3. Results And Discussions

3.1 Mean annual precipitation climatology

Rainfall is a key climatic variable in Ethiopia and particularly in the OGRB, where socio-economic activities in the region are largely based on rain-fed agriculture. Evaluation of climate models in replicating observed climatology at a local scale is a criterion for confidence in climate impact studies and analysis (Ayugi et al., 2021). Therefore, the performance of the ten RCMs, together with their ensemble mean, were compared with their ability to reproduce the observed annual climate, interannual and seasonal variability of precipitation and air temperature, and precipitation characteristics over the OGRB to select the model with the best performance at the local scale. Most regional climate models overestimated the mean annual precipitation in OGRB, especially CanRCM4 (CanESM2), RCA4 (MIROC5), and RCA4 (MPI), while CCLM4-8-17 (HadGEM2), CCLM4-8-17 (MPI), and REMO2009 (MPI) models underestimated the mean annual precipitation in the basin. In terms of BIAS statistics out of two hundred variants, the relative bias across all RCMs was found to be less than 20%, which is an acceptable relative bias range for precipitation. The maximum relative bias score was 11.95 at the Sawla station by CCLM4-8-17 (HadGEM2) and the minimum was 0.02 at the Dimeka station by CCLM4-8-17 (CNRM) (Table 2). In the upper reaches of the OGRB, especially in Emdibir, Gedo, and Gojeb, the model simulation results overestimated the climatic characteristics of precipitation, while around the Sawla, Wolaita Sodo, and Keyafer lower reaches of the basins, all regional climate models, including their ensemble mean, underestimated.

In terms of RMSE, all regional climate models captured better, except for a few stations in the upper and lower reaches of the basin, such as Emdibir, Gedo, and Hossana stations using RCA4 RCM of all families and Sawla, Wolaita-Soda and Keyafer stations of all RCMs. The highest RMSE value of 12.43 was recorded in Sawla CCLM4-8-17 (HadGEM2) and the lowest RMSE value was recorded in Assendabo CCLM4-8-17 (HadGEM2) with a magnitude of 0.52. A systematic error occurred at Assendabo station and was followed by Woliso station. A small systematic error occurred when using the ensemble at most stations other than individual RCMs. In terms of Pearson's correlation coefficient (r), Baco, Bonga, Wolaita Sodo, all regional climate model simulated annual mean precipitation is negatively correlated with observational data, except for RACMO22T (EC-EARTH) at Wolaita Sodo station, which is positively correlated with observed data. The higher positive and negative Pearson correlation coefficient (r) values were 0.88 at the Limu Genet station and − 0.85 at the Wolaita Sodo station using the CCLM4-8-17 (CNRM) and CanRCM4 (CanESM2) models, respectively. Table 2 below presents the statistical indices of the basin-wide mean annual precipitation simulations.

Table 2
Statistical indices of RCMs and their mean ensemble in the annual average precipitation simulation

Station Name	Statistical indices	RCA4				CCLM4-8-17						
		CNRM	MIROC5	MOHC-Had	MPI	CNRM	MOHC-Had	MPI	CanRCM4	RACMO22T	REMO2009	Ensemble
Arjo	r	0.32	0.29	0.44	0.28	0.27	0.15	0.27	0.46	0.41	0.34	0.37
	RMSE	1.94	1.91	1.78	1.91	1.94	2.19	2.05	2.24	1.78	2.02	1.81
	BIAS	-0.59	0.13	-0.31	0.04	0.23	-1.01	-0.80	1.42	0.11	-0.86	-0.17
Assendabo	r	0.48	0.55	0.72	0.70	0.54	0.59	0.78	0.73	0.71	0.64	0.74
	RMSE	0.87	1.09	0.59	0.76	1.22	0.66	0.52	1.70	0.98	0.68	0.65
	BIAS	-0.51	0.70	0.03	0.42	0.88	-0.06	-0.16	1.60	0.83	0.28	0.40
Baco	r	-0.27	-0.31	-0.30	-0.38	-0.47	-0.19	-0.45	-0.13	-0.27	-0.32	-0.35
	RMSE	2.35	3.33	3.36	3.43	2.55	1.57	1.90	2.77	2.67	1.86	2.43
	BIAS	1.45	2.60	2.53	2.67	1.50	-0.02	0.43	2.17	2.01	0.53	1.59
Dedo	r	0.33	0.21	0.41	0.50	0.24	0.32	0.50	0.54	0.36	0.39	0.46
	RMSE	2.12	1.89	2.13	1.68	2.38	3.09	3.04	1.77	1.98	3.03	2.05
	BIAS	-1.30	-0.37	-1.38	-0.69	-1.62	-2.61	-2.64	0.99	-1.12	-2.57	-1.33
Emdibir	r	0.16	0.25	0.50	0.40	0.40	0.23	0.25	0.72	0.05	0.54	0.39
	RMSE	4.86	7.52	5.85	6.16	1.76	1.22	1.23	1.83	1.71	1.62	3.17
	BIAS	4.50	7.25	5.59	5.87	1.31	0.27	0.33	1.65	1.20	1.30	2.93
Gedo	r	0.47	0.43	0.47	0.55	0.31	0.30	0.53	0.47	0.52	0.51	0.52
	RMSE	3.31	4.69	4.37	4.37	2.34	1.05	1.25	2.70	2.02	1.40	2.65
	BIAS	3.11	4.53	4.12	4.19	2.04	0.53	0.95	2.55	1.88	1.15	2.50
Gibe Farm	r	0.52	0.41	0.58	0.60	0.59	0.55	0.77	0.64	0.68	0.66	0.71
	RMSE	1.60	0.94	1.03	0.83	2.76	1.39	1.37	1.94	1.17	1.65	0.73
	BIAS	-1.50	-0.71	-0.89	-0.65	2.56	1.14	1.23	1.84	1.05	1.50	0.56
Gojeb	r	0.22	-0.01	-0.02	-0.03	0.11	0.10	0.20	0.30	0.28	0.14	0.15
	RMSE	2.88	3.80	2.96	3.64	3.58	2.45	2.50	6.54	3.09	2.63	3.34
	BIAS	2.50	3.38	2.46	3.20	3.21	1.98	2.02	6.36	2.79	2.18	3.01
Hossana	r	0.40	0.11	0.19	0.18	0.14	0.16	0.34	0.14	0.44	0.17	0.26
	RMSE	5.75	7.23	5.23	5.86	1.05	1.56	1.43	1.70	0.97	1.58	2.33
	BIAS	5.46	6.97	4.84	5.48	-0.21	-1.30	-1.20	1.40	0.59	-1.34	2.07
Jimma	r	0.65	0.61	0.75	0.71	0.72	0.19	0.75	0.74	0.79	0.75	0.82
	RMSE	0.80	1.11	0.78	0.85	0.90	1.87	1.74	2.10	0.59	1.69	0.62
	BIAS	-0.30	0.64	-0.38	0.31	-0.62	-1.61	-1.64	1.99	-0.11	-1.57	-0.33
Limu Genet	r	0.78	0.70	0.73	0.73	0.88	0.41	0.79	0.79	0.78	0.79	0.86
	RMSE	1.54	0.91	1.63	1.10	1.20	2.18	2.22	0.98	1.69	2.03	1.33
	BIAS	-1.38	-0.39	-1.44	-0.79	-1.08	-1.94	-2.11	0.73	-1.52	-1.91	-1.18
Woliso	r	0.59	0.46	0.66	0.74	0.67	0.76	0.70	0.73	0.51	0.77	0.80
	RMSE	1.81	0.87	0.79	0.68	2.39	0.90	1.19	1.06	0.84	1.78	0.57
	BIAS	-1.74	-0.39	-0.51	-0.46	2.15	0.57	0.87	0.91	0.58	1.61	0.36
Wolkite	r	0.51	0.40	0.54	0.47	0.45	0.35	0.52	0.42	0.54	0.51	0.54
	RMSE	1.39	1.12	1.05	1.01	1.12	1.21	1.16	1.47	0.94	0.96	0.91
	BIAS	-1.05	0.16	-0.51	-0.12	0.34	-0.60	-0.70	1.06	0.29	-0.26	-0.14
Bonga	r	-0.36	-0.69	-0.64	-0.56	-0.56	-0.53	-0.47	-0.47	-0.38	-0.51	-0.62

Station Name	Statistical indices	RCA4				CCLM4-8-17						
		CNRM	MIROC5	MOHC-Had	MPI	CNRM	MOHC-Had	MPI	CanRCM4	RACMO22T	REMO2009	Ensemble
	RMSE	1.89	1.66	1.92	1.68	2.00	1.77	1.86	3.73	1.23	1.65	1.49
	BIAS	-1.37	-0.23	-1.12	-0.47	0.60	-1.11	-0.87	3.30	-0.49	-0.68	-0.24
Morka	r	0.51	0.20	0.45	0.54	0.42	0.48	0.45	0.53	0.48	0.46	0.61
	RMSE	1.49	1.44	1.82	1.52	0.82	1.96	1.55	1.43	0.70	1.07	1.00
	BIAS	-1.40	-1.29	-1.74	-1.43	-0.43	-1.89	-1.43	1.29	0.39	-0.89	-0.88
Sawla	r	0.55	0.26	0.75	0.57	0.47	0.42	0.44	0.57	0.48	0.69	0.74
	RMSE	9.58	9.86	10.79	9.57	10.33	12.43	11.67	8.47	8.60	11.18	10.22
	BIAS	-9.06	-9.24	-10.36	-9.07	-9.82	-11.95	-11.19	-7.86	-7.93	-10.71	-9.72
Wolaita Sodo	r	-0.43	-0.37	-0.80	-0.62	-0.24	-0.81	-0.65	-0.85	0.35	-0.76	-0.83
	RMSE	9.43	9.36	9.43	9.32	9.90	9.80	9.47	9.77	9.08	9.43	9.49
	BIAS	-9.12	-9.08	-9.05	-8.99	-9.65	-9.46	-9.14	-9.41	-8.85	-9.07	-9.18
Dimeka	r	0.06	-0.05	-0.02	-0.12	-0.03	-0.23	0.01	-0.02	0.21	0.10	-0.02
	RMSE	1.56	1.35	1.00	1.66	1.19	1.58	1.25	2.15	1.70	1.34	0.93
	BIAS	1.07	0.76	-0.32	1.12	0.02	-1.32	-0.80	1.84	1.47	-1.04	0.28
Jinka	r	0.20	-0.07	0.50	0.30	0.02	0.14	0.34	0.29	0.15	0.51	0.37
	RMSE	1.37	1.43	2.16	1.20	1.73	3.10	2.48	1.18	1.15	2.57	1.43
	BIAS	-0.99	-1.06	-2.05	-0.73	-1.20	-3.00	-2.36	0.70	0.76	-2.48	-1.24
Keyafer	r	0.46	-0.16	0.19	0.50	0.26	0.02	0.26	0.15	0.07	0.40	0.41
	RMSE	9.77	9.93	10.85	9.51	10.02	11.78	11.14	8.21	8.15	11.25	10.04
	BIAS	-9.49	-9.56	-10.55	-9.24	-9.71	-11.50	-10.86	-7.80	-7.74	-10.98	-9.74

3.2 Average annual air temperature climate

3.2.1. Maximum mean annual air temperature climate

The performance of all models in capturing the air temperature pattern was superior, while the RCA4 (HadGEM2) and CCLM4-8-17 (HadGEM2) models poorly reproduced the pattern of maximum annual mean air temperature in the basin. Almost all RCMs, including the ensemble mean, underestimated the maximum annual mean air temperature in the basin, except for REMO2009 (MPI), which was overestimated. The RACMO22T (EC-EARTH) and CCLM4-8-17 (CNRM) models simulated the lowest maximum annual mean air temperature in the study area than the other RCMs considered in this study. The minimum observed bias was 0.02ºC at Dimeka and Bako stations using CCLM4-8-17 (CNRM) and CCLM4-8-17 (HadGEM2) models, followed by 0.03ºC at Assendabo station using CCLM4-8-17 (HadGEM2). However, the maximum observed bias was 11.95ºC at Sawla station from CCLM4-8-17 (HadGEM2). All RCMs depicted high negative bias values at Sawla, Wolaita Sodo, and Keyafer stations, indicating that the models were highly biased in these areas. In addition, the RMSE value shows a high magnitude at Sawla, Wolaita Sodo, and Keyafer stations, indicating that the model poorly reproduces the observation. There was a negative correlation between observed and simulated annual mean maximum temperatures by all RCMs at Bongo, Bako, except for RACMO22T (EC-EARTH) at Wolaita Sodo stations. At most stations, the RCM showed a positive correlation in the simulation of maximum annual mean air temperature (Table 3).

Table 3
Statistical indicators in the simulation of the average annual maximum air temperature.

Station Name	Statistical indices	RCA4				CCLM4-8-17						
		CNRM	MIROC5	MOHC-Had	MPI	CNRM	MOHC-Had	MPI	CanRCM4	RACMO22T	REMO2009	Ensemble
Arjo	r	0.32	0.29	0.44	0.28	0.27	0.15	0.27	0.46	0.41	0.34	0.37
	RMSE	1.94	1.91	1.78	1.91	1.94	2.19	2.05	2.24	1.78	2.02	1.81
	BIAS	-0.59	0.13	-0.31	0.04	0.23	-1.01	-0.80	1.42	0.11	-0.86	-0.17
Assendabo	r	0.48	0.55	0.72	0.70	0.54	0.59	0.78	0.73	0.71	0.64	0.74
	RMSE	0.87	1.09	0.59	0.76	1.22	0.66	0.52	1.70	0.98	0.68	0.65
	BIAS	-0.51	0.70	0.03	0.42	0.88	-0.06	-0.16	1.60	0.83	0.28	0.40
Baco	r	-0.27	-0.31	-0.30	-0.38	-0.47	-0.19	-0.45	-0.13	-0.27	-0.32	-0.35
	RMSE	2.35	3.33	3.36	3.43	2.55	1.57	1.90	2.77	2.67	1.86	2.43
	BIAS	1.45	2.60	2.53	2.67	1.50	-0.02	0.43	2.17	2.01	0.53	1.59
Dedo	r	0.33	0.21	0.41	0.50	0.23	0.32	0.50	0.54	0.36	0.39	0.46
	RMSE	2.12	1.89	2.13	1.68	2.38	3.09	3.04	1.77	1.98	3.03	2.05
	BIAS	-1.30	-0.37	-1.38	-0.69	-1.62	-2.61	-2.64	0.99	-1.12	-2.57	-1.33
Emdibir	r	0.16	0.25	0.50	0.40	0.40	0.23	0.25	0.72	0.05	0.54	0.39
	RMSE	4.86	7.52	5.85	6.16	1.76	1.22	1.23	1.83	1.71	1.62	3.17
	BIAS	4.50	7.25	5.59	5.87	1.31	0.27	0.33	1.65	1.20	1.30	2.93
Gedo	r	0.47	0.43	0.47	0.55	0.31	0.30	0.53	0.47	0.52	0.51	0.52
	RMSE	3.31	4.69	4.37	4.37	2.34	1.05	1.25	2.70	2.02	1.40	2.65
	BIAS	3.11	4.53	4.12	4.19	2.04	0.53	0.95	2.55	1.88	1.15	2.50
Gibe Farm	r	0.52	0.41	0.58	0.60	0.59	0.55	0.77	0.64	0.67	0.66	0.71
	RMSE	1.60	0.94	1.03	0.83	2.76	1.39	1.37	1.94	1.17	1.65	0.73
	BIAS	-1.50	-0.71	-0.89	-0.65	2.56	1.14	1.23	1.84	1.05	1.50	0.56
Gojeb	r	0.22	-0.01	-0.02	-0.03	0.11	0.10	0.20	0.30	0.28	0.14	0.15
	RMSE	2.88	3.80	2.96	3.64	3.58	2.45	2.50	6.54	3.09	2.63	3.34
	BIAS	2.50	3.38	2.46	3.20	3.21	1.98	2.02	6.36	2.79	2.18	3.01
Hossana	r	0.40	0.11	0.19	0.18	0.14	0.16	0.34	0.14	0.43	0.17	0.26
	RMSE	5.75	7.23	5.23	5.86	1.05	1.56	1.43	1.70	0.97	1.58	2.33
	BIAS	5.46	6.97	4.84	5.48	-0.21	-1.30	-1.20	1.40	0.59	-1.34	2.07
Jimma	r	0.65	0.61	0.75	0.71	0.72	0.19	0.75	0.74	0.79	0.75	0.82
	RMSE	0.80	1.11	0.78	0.85	0.90	1.87	1.74	2.10	0.59	1.69	0.62
	BIAS	-0.30	0.64	-0.38	0.31	-0.62	-1.61	-1.64	1.99	-0.11	-1.57	-0.33
Limu Genet	r	0.78	0.70	0.73	0.73	0.88	0.41	0.78	0.79	0.78	0.79	0.86
	RMSE	1.54	0.91	1.63	1.10	1.20	2.18	2.22	0.98	1.69	2.03	1.33
	BIAS	-1.38	-0.39	-1.44	-0.79	-1.08	-1.94	-2.11	0.73	-1.52	-1.91	-1.18
Woliso	r	0.59	0.46	0.66	0.73	0.67	0.75	0.70	0.73	0.51	0.77	0.80
	RMSE	1.81	0.87	0.79	0.68	2.39	0.90	1.19	1.06	0.84	1.78	0.57
	BIAS	-1.74	-0.39	-0.51	-0.46	2.15	0.57	0.87	0.91	0.58	1.61	0.36
Wolkite	r	0.51	0.40	0.54	0.47	0.45	0.35	0.51	0.42	0.54	0.51	0.54
	RMSE	1.39	1.12	1.05	1.01	1.12	1.21	1.16	1.47	0.94	0.96	0.91
	BIAS	-1.05	0.16	-0.51	-0.12	0.34	-0.60	-0.70	1.06	0.29	-0.26	-0.14
Bonga	r	-0.36	-0.69	-0.64	-0.56	-0.56	-0.53	-0.47	-0.47	-0.38	-0.51	-0.62

Station Name	Statistical indices	RCA4				CCLM4-8-17						
		CNRM	MIROC5	MOHC-Had	MPI	CNRM	MOHC-Had	MPI	CanRCM4	RACMO22T	REMO2009	Ensemble
	RMSE	1.89	1.66	1.92	1.68	2.00	1.77	1.86	3.73	1.23	1.65	1.49
	BIAS	-1.37	-0.23	-1.12	-0.47	0.60	-1.11	-0.87	3.30	-0.49	-0.68	-0.24
Morka	r	0.51	0.20	0.45	0.54	0.42	0.48	0.45	0.53	0.48	0.46	0.61
	RMSE	1.49	1.44	1.82	1.52	0.82	1.96	1.55	1.43	0.70	1.07	1.00
	BIAS	-1.40	-1.29	-1.74	-1.43	-0.43	-1.89	-1.43	1.29	0.39	-0.89	-0.88
Sawla	r	0.55	0.26	0.75	0.56	0.47	0.42	0.44	0.58	0.48	0.69	0.74
	RMSE	9.58	9.86	10.79	9.57	10.33	12.43	11.67	8.47	8.60	11.18	10.22
	BIAS	-9.06	-9.24	-10.36	-9.07	-9.82	-11.95	-11.19	-7.86	-7.93	-10.71	-9.72
Wolaita Sodo	r	-0.43	-0.37	-0.80	-0.62	-0.24	-0.81	-0.65	-0.85	0.35	-0.76	-0.83
	RMSE	9.43	9.36	9.43	9.32	9.90	9.80	9.47	9.77	9.08	9.43	9.49
	BIAS	-9.12	-9.08	-9.05	-8.99	-9.65	-9.46	-9.14	-9.41	-8.85	-9.07	-9.18
Dimeka	r	0.06	-0.05	-0.02	-0.12	-0.03	-0.23	0.01	-0.02	0.21	0.10	-0.02
	RMSE	1.56	1.35	1.00	1.66	1.19	1.58	1.25	2.15	1.70	1.34	0.93
	BIAS	1.07	0.76	-0.32	1.12	0.02	-1.32	-0.80	1.84	1.47	-1.04	0.28
Jinka	r	0.20	-0.07	0.50	0.30	0.02	0.15	0.34	0.29	0.15	0.50	0.37
	RMSE	0.103	0.104	0.14	0.109	0.067	0.171	0.116	0.085	0.065	0.245	0.106
	BIAS	-0.99	-1.06	-2.05	-0.73	-1.20	-3.00	-2.36	0.70	0.76	-2.48	-1.24
Keyafer	r	0.46	-0.16	0.19	0.50	0.26	0.02	0.26	0.15	0.07	0.40	0.41
	RMSE	9.77	9.93	10.85	9.51	10.02	11.78	11.14	8.21	8.15	11.25	10.04
	BIAS	-9.49	-9.56	-10.55	-9.24	-9.71	-11.50	-10.86	-7.80	-7.74	-10.98	-9.74

3.2.2. Minimum average annual air temperature climate

The performance of almost all models was quite good in simulating the minimum annual mean air temperature at Emdibir, Asendabo, Jimma, Bako, Dedo, Jinka, Sawla, Gedo, and Wolkite stations, but was highly biased around Wolaita-Soda, Gojeb, Woliso, Arjo, Dimeka and Gibe Farm stations. The RMSE values also confirm the same observation with different magnitudes. RCA4 (MPI) and CCLM4-8-17 (MPI) performed better than all individual RCMs at most stations. The largest observed bias was 18.44ºC and 18.24ºC using RCA4 (HadGEM2) and CCLM4-8-17 (HadGEM2), and the RMSE values were 18.45 and 18.25 using RCA4 (HadGEM2) and CCLM4-8-17 (HadGEM2) respectively at Wolaita Sodo station. Almost all models overestimated the minimum annual average air temperature compared to observational data. Moreover, the simulation results of the CCLM4-8-17 (HadGEM2) and CCLM4-8-17 (MPI) models significantly overestimated the minimum annual mean air temperature compared to other models. Mostly, the simulation results had a positive correlation with the observational data, but at Wolaita Sodo station, the simulation results showed a negative correlation with the observed data (Table 4).

Table 4
Statistical indicators in reproducing the average annual minimum air temperature.

Station Name	Statistical indices	RCA4				CCLM4-8-17						
		CNRM	MIROC5	MOHC-Had	MPI	CNRM	MOHC-Had	MPI	CanRCM4	RACMO22T	REMO2009	Ensemble
Arjo	r	-0.32	0.15	-0.59	-0.32	-0.37	-0.55	0.40	-0.47	-0.22	0.26	-0.37
	RMSE	9.93	10.85	11.04	10.68	11.42	12.65	12.26	9.24	8.77	10.28	10.67
	BIAS	7.90	9.18	9.11	8.76	9.75	11.12	10.86	6.85	6.47	8.54	8.85
Assendabo	r	0.02	0.05	-0.36	-0.25	-0.24	-0.24	0.20	-0.31	0.12	0.29	-0.19
	RMSE	3.83	3.13	3.43	3.40	3.21	2.97	2.80	5.19	5.48	2.89	3.46
	BIAS	-2.63	-1.39	-1.49	-1.70	-1.49	-0.41	-0.71	-4.20	-4.75	-1.14	-1.99
Baco	r	-0.05	-0.34	-0.17	-0.29	-0.38	-0.21	0.31	-0.26	-0.16	0.12	-0.25
	RMSE	5.63	5.51	5.45	5.57	5.44	5.43	5.19	6.19	6.66	5.52	5.49
	BIAS	-1.83	-0.45	-0.57	-0.86	-0.51	0.64	0.43	-2.94	-3.97	-1.70	-1.18
Dedo	r	0.26	0.10	0.13	0.00	0.37	0.30	0.25	-0.15	0.22	0.24	0.28
	RMSE	4.64	5.12	5.03	4.98	5.13	5.96	5.68	4.84	4.74	4.61	4.85
	BIAS	0.81	2.18	1.99	1.68	2.36	3.83	3.40	-0.08	-1.14	0.78	1.58
Emdibir	r	0.02	0.01	-0.38	0.09	-0.14	-0.38	0.36	0.02	0.33	0.29	-0.02
	RMSE	5.97	5.44	5.72	5.51	5.45	5.39	5.10	6.60	7.03	5.92	5.68
	BIAS	-3.05	-1.72	-1.85	-2.07	-1.71	-0.63	-1.00	-4.13	-4.90	-3.14	-2.42
Gedo	r	-0.17	0.38	-0.55	-0.40	-0.26	-0.66	0.43	-0.21	-0.04	-0.26	-0.35
	RMSE	2.15	2.59	2.89	2.66	2.97	3.82	3.34	2.33	2.47	2.24	2.38
	BIAS	0.33	1.77	1.49	1.27	2.06	2.95	2.75	-0.75	-1.35	-0.28	1.02
Gibe Farm	r	-0.02	-0.20	-0.20	0.10	0.00	-0.24	0.10	-0.13	-0.18	0.03	-0.16
	RMSE	11.41	12.08	11.96	11.75	11.31	12.05	11.76	10.41	10.14	12.06	11.42
	BIAS	6.22	7.20	7.06	6.89	6.05	7.17	6.91	3.91	3.23	7.36	6.20
Gojeb	r	-0.12	0.13	-0.02	-0.19	-0.09	0.10	-0.04	-0.08	-0.20	-0.18	-0.12
	RMSE	12.24	13.65	13.46	13.12	13.52	14.94	14.54	12.19	9.97	12.83	13.04
	BIAS	12.19	13.59	13.39	13.06	13.47	14.90	14.49	12.11	9.90	12.77	12.99
Hossana	r	0.07	0.11	-0.01	0.43	0.38	0.02	0.47	0.10	0.59	0.61	0.44
	RMSE	5.05	5.40	5.44	5.13	6.12	7.13	6.60	4.98	4.86	4.74	5.28
	BIAS	0.77	2.11	2.03	1.80	3.67	5.07	4.51	0.12	-0.42	0.04	1.97
Jimma	r	0.14	0.65	-0.55	-0.47	0.23	-0.14	0.63	-0.63	0.12	0.39	-0.03
	RMSE	3.05	1.72	2.49	2.52	1.77	1.47	1.11	4.13	4.88	3.04	2.40
	BIAS	-2.74	-1.38	-1.56	-1.87	-1.19	0.28	-0.15	-3.63	-4.69	-2.77	-1.97
Limu Genet	r	0.55	0.23	-0.22	0.28	0.17	-0.10	0.82	-0.33	0.48	0.79	0.31
	RMSE	8.29	8.93	9.13	8.67	8.88	9.69	9.17	8.56	7.93	8.32	8.66
	BIAS	2.85	4.27	3.99	3.73	3.99	5.39	5.09	1.70	1.12	3.43	3.56
Woliso	r	-0.04	0.49	-0.70	-0.34	-0.53	-0.77	0.11	-0.24	-0.15	0.40	-0.31
	RMSE	11.93	13.09	12.89	12.73	11.75	12.77	12.42	10.21	8.94	14.11	12.08
	BIAS	11.92	13.07	12.88	12.72	11.75	12.75	12.41	10.20	8.93	14.10	12.07
Wolkite	r	-0.11	0.04	-0.48	-0.04	-0.10	-0.50	0.31	-0.37	0.28	0.46	-0.18
	RMSE	3.90	4.15	4.44	4.07	4.12	4.82	4.32	4.36	4.21	4.02	4.00
	BIAS	0.23	1.48	1.37	1.17	1.37	2.46	2.16	-1.33	-1.88	1.73	0.88
Bonga	r	-0.12	0.32	-0.77	-0.43	-0.58	-0.29	0.40	-0.74	-0.55	0.48	-0.46

Station Name	Statistical indices	RCA4				CCLM4-8-17						
		CNRM	MIROC5	MOHC-Had	MPI	CNRM	MOHC-Had	MPI	CanRCM4	RACMO22T	REMO2009	Ensemble
	RMSE	4.00	2.78	3.39	3.48	3.20	2.33	2.38	3.29	6.05	2.34	3.25
	BIAS	-3.51	-2.16	-2.33	-2.66	-2.47	-1.29	-1.64	-2.40	-5.69	-1.64	-2.58
Morka	r	-0.51	0.54	-0.35	-0.53	0.16	0.32	-0.14	-0.23	-0.06	-0.01	-0.17
	RMSE	6.71	5.09	5.74	6.01	4.54	3.32	3.90	6.99	7.51	4.47	5.33
	BIAS	-5.87	-4.35	-4.70	-4.94	-3.45	-1.63	-2.38	-6.21	-6.87	-3.27	-4.37
Sawla	r	0.05	0.31	-0.35	0.14	0.17	-0.01	0.46	-0.38	-0.14	0.35	0.10
	RMSE	1.16	0.88	0.92	0.67	0.64	2.45	1.65	2.45	3.46	0.71	0.47
	BIAS	-1.05	0.36	0.08	-0.18	0.47	2.38	1.61	-2.33	-3.43	-0.57	-0.26
Wolaita Sodo	r	-0.16	-0.41	-0.22	-0.12	-0.16	-0.11	-0.13	-0.27	-0.25	-0.10	-0.20
	RMSE	17.38	18.12	18.45	17.80	17.20	18.25	17.43	17.80	16.91	17.66	17.70
	BIAS	17.35	18.08	18.44	17.76	17.16	18.24	17.37	17.77	16.89	17.62	17.67
Dimeka	r	0.06	0.33	-0.24	-0.04	0.07	0.12	0.16	-0.13	-0.33	0.14	0.05
	RMSE	11.05	11.98	12.17	11.72	12.01	13.09	12.92	10.02	9.62	11.20	11.49
	BIAS	7.28	8.83	8.72	8.20	8.66	10.12	9.92	5.42	4.51	7.54	7.92
Jinka	r	0.17	0.59	-0.20	-0.05	0.44	0.48	0.42	-0.37	-0.13	0.34	0.34
	RMSE	1.57	2.29	2.56	2.14	2.28	3.92	3.42	2.38	2.95	1.51	1.79
	BIAS	0.58	1.96	1.92	1.43	1.85	3.70	3.14	-1.59	-2.50	0.62	1.11
Keyafer	r	0.19	0.12	-0.03	0.30	0.47	0.48	0.50	-0.19	0.34	0.44	0.45
	RMSE	3.21	4.61	4.56	4.03	4.42	6.25	5.69	1.49	0.86	3.22	3.70
	BIAS	3.08	4.46	4.42	3.93	4.35	6.19	5.63	0.91	-0.01	3.12	3.61

3.3. Mean monthly climatic variables cycle

3.3.1. Mean monthly precipitation cycle

In terms of rainfall regime, in OGRB, the main rainy months fall on JJAS with a monomodal rainfall pattern (Fig. 2). The basin receives rainfall in two main seasons, the small rainy season (March-May) locally known as 'Belg', and the main rainy season (June-September) locally known as 'Kiremt', and the dry season (November-February), locally known as 'Bega'. In the upper reaches of the basin, most RCMs reproduce the main rainy months in JJAS, similar to the observed, peak rainfall in July. Although the REMO2009 (MPI) recorded the main rainy months in JJAS, the peak was shifted to June. On the other hand, in the upper reaches, the common error in the model simulation outputs of CCLM4-8-17 (CNRM), RCA4 (MIROC5), and RACMO22T (EC-EARTH) was simulated with a double peak in different months from April to September, however, the observed rainfall at the station reflected only one peak in July. The RCA4 (HadGEM2) and CCLM4-8-17 (HadGEM2) overestimated precipitation in dry months and underestimated it in wet months, while the lowest value of precipitation was simulated by this model in wet months than all other models considered. The RCA4 family of all driving models, except RCA4 (HadGEM2), showed high interannual variation, estimating relatively very high precipitation in wet months and low precipitation in dry months, mainly RCA4 (MPI). All the RCMs' simulated rainfall was reasonably better in the dry months than the wet months except RCA4 (HadGEM2) and CCLM4-8-17 (HadGEM2). The two models were found to be unable to capture and reproduce both the magnitude and climate pattern of basin-wide precipitation. Figure 2 exhibited the mean monthly precipitation cycles for most of the observed stations, the ten RCMs, the multi-model ensemble, and the basin-wide mean monthly precipitation cycle. However, in the middle and lower reaches of the basins, two rainfall peaks betweenMarch–May (MAM) and August–November (ASON) were observed. In this reach, most models repeat the peak of precipitation between (March-June) in May, while CanRCM4 (CanESM2), RCA4 (MIROC5), and observations show in April. Likewise, between (August–November) REMO2009 (MPI) and RCA4 (MIROC5) show a peak in September, unlike the other models observed in October.

Overall, in the OGRB, all RCMs performed better in simulating precipitation in dry months than in wet months, but RCA4 (HadGEM2) and CCLM4-8-17 (HadGEM2) performed poorly in the basin. During the wet months, most models simulated overestimated precipitation, except for RCA4 (HadGEM2), CCLM4-8-17 (CNRM), CCLM4-8-17 (HadGEM2), and CCLM4-8-17 (MPI), which showed underestimated precipitation.

3.3.2. Mean monthly maximum and minimum air temperature cycles

a. Mean monthly maximum air temperature cycle

All RCMs except REMO2009 (MPI) underestimated the mean maximum air temperature for all months. RACMO22T (EC-EARTH) and CCLM4-8-17 (CNRM) were weak in simulating the maximum air temperature, while REMO2009 (MPI) modeled it quite reasonably and captured the cycle better throughout the river basin

(Fig. 3). All models simulated maximum monthly air temperatures from January to April and from August to December, but RCA4 (HadGEM2) and CCLM4-8-17 (HadGEM2) reproduced a minimum during this month. The maximum air temperatures of all models, including their ensemble mean and observed, decreased between May and September, and the minimums fell in July, while RCA4 (HadGEM2) and CCLM4-8-17 (HadGEM2) replicated the increase, with a maximum in July and it was not possible to reproduce the average monthly cycle of maximum air temperature throughout the basin. Figure 3 depicts the selected station's mean monthly and mean annual cycle of maximum air temperature over the entire river basin.

b. Mean monthly minimum air temperature cycle

All RCMs overestimated the average monthly minimum air temperature for several months; however, an underestimation was detected between February and March with varying magnitudes of air temperature. CCLM4-8-17 (HadGEM2) and CCLM4-8-17 (MPI) replicated the minimum air temperature poorly, while RACMO22T (EC-EARTH) and CanRCM4 (CanESM2) simulated better than the other models. All models captured the cycle better throughout the river basin, except RCA4 (HadGEM2) and CCLM4-8-17 (HadGEM2). The models estimated high values between January and April and August to October, with minimum air temperatures progressively increasing from January to May but decreasing from September to October (Fig. 4). Figure 4 portrays some of the stations' mean monthly and mean annual cycles of minimum air temperature over the entire river basin.

3.4. Annual and seasonal climate variability

3.4.1. Annual and seasonal rainfall variability

The variability in the annual and June to September (JJAS) seasonal rainfall was detected less than 20% except for the RCA4 (HadGEM2) and CCLM4-8-17 (HadGEM2) model simulation outputs (Table 4). The CV values of MAM seasonal precipitation varied in the range of 20–30 moderate categories, except for the RCA4 and CCLM4-8-17 model family from all deriving models considered in this study. RCMs of all RCA4 families except RCA4 (MPI) and the CCLM4-8-17 family of all GCMs considered, the ensemble mean and observed overestimated interannual variability of precipitation compared to other models. RCA4 (HadGEM2) and CCLM4-8-17 (HadGEM2) performed poorly in capturing the seasonal variability of JJAS precipitation. In addition, during the MAM seasons, all RCM simulation outputs except RACMO22T (EC-EARTH), REMO2009 (MPI), CanRCM4 (CanESM2), and the ensemble mean overestimated the seasonal variability of precipitation in the basin. The interannual variability of the seasonal precipitation anomalies was considered over the entire basin and presented in Fig. 5 for the observed precipitation, the ten RCMs, and their ensemble mean.

Overall, the replicated model precipitation exhibited more variability in the MAM season (Belg) than in the JJAS season (Kiremt), implying that the variability of the summer season precipitation was reasonably low. The variability in the mean ensemble of JJAS and MAM was found to be smaller compared to the CV value of the corresponding observation. Multimodel ensemble means data were found to be moderately consistent with observational data for the years considered and consistent with studies of other scientists in different locations (Demissie & Sime, 2021; Dibaba et al., 2019; Gadissa et al., 2018).

3.4.2. Mean annual and seasonal air temperature variability

The average annual maximum and minimum of air temperature variability were within the range of low variability. In addition, the seasonal maximum and minimum variability of air temperature was less than 20%. The variability of minimum and maximum air temperatures in MAM was found to be high compared to the JJAS season. The variability of the maximum air temperature of the RCMs was slightly higher compared to the minimum air temperature. The interannual variability of minimum and maximum temperature was found to be smaller compared to the seasonal variability of the JJAS and MAM seasons in the basin (Table 5).

Table 5
Coefficient of variation (CV) for the seasonal and annual precipitation and temperature.

Parameters	Seasons	RCA4				CCLM4-8-17							
		CNRM	MIROC5	MOHC-Had	MPI	CNRM	MOHC-Had	MPI	CanRCM4	RACMO22T	REMO2009	Ensemble	Ob
Rainfall	JJAS	7.92	17.19	81.00	9.04	12.48	54.90	16.29	8.22	10.02	14.17	8.09	14
	MAM	33.90	30.58	116.9	38.14	30.13	104.66	33.77	27.11	23.89	28.69	22.96	24
	Annual	10.18	11.21	24.34	7.90	11.79	20.61	14.07	6.49	7.13	8.20	18.02	9.1
MaxTMP	JJAS	7.83	6.79	8.09	8.17	7.07	9.07	7.40	7.12	7.18	7.61	7.31	7.1
	MAM	15.97	15.20	15.90	15.92	15.37	16.65	15.04	15.04	17.25	15.91	15.50	15
	Annual	2.55	3.36	1.78	2.99	4.09	2.00	4.41	3.74	1.93	3.04	2.50	2.1
Mini TMP	JJAS	7.44	6.45	7.35	7.95	7.05	7.60	7.45	6.67	7.27	7.68	6.96	11
	MAM	16.42	16.00	18.18	16.47	15.75	16.24	15.96	16.98	16.51	15.72	16.10	15
	Annual	2.41	3.96	4.21	3.82	1.76	2.12	2.09	4.63	2.37	2.91	1.74	13

The climate parameters indicated in Table 4, Max TMP designates Maximum Temperature and Mini TMP designates Minimum Temperature.

In addition, seasonal anomalies from June to September (JJAS) and March to May (MAM) based on interannual variability were used to analyze minimum and maximum air temperatures over time. Anomaly calculations are made relative to the minimum and maximum average air temperatures obtained over the

full 20-year period 1986–2005. The data were expressed as standardized anomalies to account for the seasonal variation that exists in the data set. The area-averaged minimum and maximum air temperature anomalies were standardized by the standard deviation obtained over 20 years.

Most models and the observed annual maximum air temperature produced a negative anomaly between 1986 to 1990 and 1996 to 1998. Also, in between 1991 and 1995 in most RCMs negative anomalies were replicated, but the observed was shown a positive anomaly except for the year 1993, which showed a negative anomaly and agreed with all model simulations except RCA4 (MIROC5). Observations show considerable variation, but most models replicated positive anomalies between 1999 and 2005 in maximum air temperature. The JJAS and MAM seasonal maximum air temperature anomalies showed an increase in air temperature between 1986 and 2005, except for a few models, but in 2004, observed and all models showed negative anomalies. The RCA4 (MIROC5) showed significant variability compared to other RCMs in replicating JJAS and CanRCM4 (CanESM2) MAM seasonal annual maximum air temperature anomalies.

Annual minimum air temperature in 1986 and the period from 1992 to 1997, most of the simulated models produced negative anomalies, while in the period from 1989 to 1990 and from 2000 to 2002 and 2004, positive anomalies were observed. Model-based variations in minimum air temperature differed slightly from observed values in 1986, 1994–1988, and 2003 for the JJAS and MAM seasons mutually and between 1987–1988, 1998–1999, and 2003 annually. In JJAS, all RCMs simulate the minimum air temperature better. Seasonal variation of minimum air temperature increased continuously from 1987 to 1992 and from 1999 to 2002 in spring and summer. The JJAS and MAM season produced negative anomalies between 2004 and 2005 in all models and observed. Figure 6 portrays the interannual variability of seasonal minimum and maximum air temperature anomalies over the entire basin for observed minimum and maximum air temperatures, ten RCMs, and their mean ensemble.

3.5. Observed and RCMs event characteristics

To analyze the characteristics of extreme precipitation, the areal precipitation over the entire basin for the period from 1986 to 2005 was used. The distribution of observed precipitation and RCMs simulation by different boundary conditions for the period from 1986 to 2005 showed a clear difference between the models. The cumulative distribution of maximum extreme value type I was used. RCA4 (MIROC5) simulated the distribution of extreme precipitation reasonably associated with other models (Fig. 7). The probability of heavy precipitation was high in all models, while in the observational data there was no probability of very extreme precipitation greater than 21.5 mm/day. All RCMs overestimated the return period, including their ensemble mean (Fig. 8). The skill of the multi-model ensemble RACMO22T (EC-EARTH) and RCA4 (CNRM) replicated the return period much more reasonable than the other models, with a smaller error in magnitude. The model simulations of RCA4 (MIROC5), CCLM4-8-17 (HadGEM2), and CCLM4-8-17 (CNRM) significantly overestimated the return period with the largest error, respectively (Fig. 8). The findings of the study were in agreement by (Demissie & Sime, 2021).

3.6. Spatial analysis of mean annual precipitation

In the basin, the amount of precipitation varies both in quantity and space due to the complex topography of the regions. The RCMs and observed precipitation data from 1986 to 2005 were used to examine the spatial variation of precipitation across the basin (Fig. 9). The annual mean minimum modeled value was 0.27 mm and 0.49 mm at Dimeka and Jinka stations using CCLM4-8-17 (HadGEM2). The RCMs of the RCA4 family simulated the maximum mean annual precipitation ranging from 7.5 mm to 10.4 mm at the Emdibir and Hosana stations. The multi-model ensemble reproduced the maximum annual mean precipitation values of 5.74 mm at the Emdibir station and the minimum of 1.47 mm at the Wolaita Sodo stations. The CCLM4-8-17 of all families used and REMO2009 (MPI) reproduce the maximum annual mean rainfall at Woliso station and the minimum at Dimeka station, except CCLM4-8-17 (CNRM) which simulates the minimum at Wolaita Sodo station. On the other hand, CanRCM4 (CanESM2) and RACMO22T (EC-EARTH) reproduce a maximum at Bonga and Bako stations and a minimum at Wolaita Sodo station. However, the observed actual station data yielded high mean annual precipitation values at Dedo station with 5.27 mm, followed by 4.89 mm at Limu-Genet station and minimum values of 0.94 mm and 1.65 mm at Gojeb and Dimeka stations respectively (Fig. 9). The average annual maximum precipitation was simulated in the upper reaches of the basin as compared to the lower reaches. Almost all models, including their mean ensemble, simulated minimal precipitation in the lower reaches of the basin and moderate precipitation in the middle reaches. Multi-model ensemble and RACMO22T (EC-EARTH) replicated reasonably the mean annual precipitation distribution than other models. Figure 9 illustrates the spatial mean annual precipitation distribution from 1986 to 2005 for observed, ten RCMs and their mean ensemble over the entire basin. Overall, the results of the investigation confirm the difference between RCMs in capturing climate conditions at both spatial and temporal scales. The result is consistent with other findings in different regions of Ethiopia (Demissie & Sime, 2021; Dibaba et al., 2019; Girma et al., 2022).

4. Conclusions

In this study, the performance of the CORDEX Africa RCM in reproducing precipitation and air temperature was evaluated using observed data as a reference for the baseline period from 1986 to 2005. The performance of the RCM was found variable at both spatial and temporal scales. All RCMs performed better in simulating precipitation in dry months than in wet months, but RCA4 (HadGEM2) and CCLM4-8-17 (HadGEM2) performed poorly in capturing both the magnitude and climatological cycle of precipitation over the basin. In the wet months, most models replicated overestimated precipitation, except for RCA4 (HadGEM2), CCLM4-8-17 (CNRM), CCLM4-8-17 (HadGEM2), and CCLM4-8-17 (MPI), which exhibited underestimated precipitation. In both the precipitation and air temperature model simulations, the multi-model ensemble data agree reasonably better with the observations compared to the individual RCMs. Interannual and seasonal variability of both precipitation and air temperature occurred in the lowest categories over the basin. All RCMs, including their ensemble mean, overestimated areal precipitation extremes and return periods. RCMs are superior at simulating maximum air temperatures than minimums. Almost all RCMs simulation output overestimated the annual mean minimum air temperature at most stations, except for May to February, and underestimated the annual mean maximum temperature, except for REMO2009 (MPI), which was overestimated compared to the basin-wide observational data. The simulation results of the CCLM4-8-17 (HadGEM2) and CCLM4-8-17 (MPI) models significantly overestimated the minimum annual average air temperature compared to other models. The RACMO22T (EC-EARTH) model was found superior in capturing the minimum air temperature, while it was found to be weak and followed by CCLM4-8-17 (CNRM) in determining the magnitude of the maximum annual mean air temperature in the study area than the

others. In general, the RCMs performing better in replicating observed climate conditions were RACMO22T (EC-EARTH), CCLM4-8-17 (CNRM), RCA4 (CNRM), CCLM4-8-17 (MPI), REMO2009 (MPI), and RCA4 (MPI), while the RCA4 (HadGEM2) and CCLM4-8-17 (HadGEM2) models performed the worst in replicating the OGRB climatology.

Overall, the results of this performance evaluation exhibited that the use of the CORDEX-Africa regional climate models simulation outputs at the locale and finer scale, is important for analyzing the effects of climate change in the individual regions of East Africa, particularly in the OGRB, Ethiopia. In addition, the investigation detected systematic deviations in model performance, and thus it is indispensable to be alert to these boundaries before using RCM simulation results to investigate climate change impacts on groundwater and surface water resources, agricultural production, soil loss estimation, reservoir operation, and hydropower production. The differences in the RCM performance robustly portrayed the significance of bias adjustments in RCMs simulation results before employing them for climate change impact and adaptation studies.

Declarations

Author contribution statement

"YM Conceived and designed the study, performed the data analysis, and wrote the manuscript; BA reviewed the statistical analysis and substantially revised the text during the review process and gave substantial contributions to the manuscript; MD reviewed the statistical analysis and substantially revised the text during the review process and coordinated the study and gave substantial contributions to the manuscript. All authors read and approved the final manuscript."

Funding statement

The authors did not receive support from any organization for the submitted work.

Conflicts of interest

The authors have no conflicts of interest to declare that are relevant to the content of this article.

Ethics approval

Not applicable.

Consent to participate

Not applicable.

Consent for publication

Not applicable

Data availability statement

The data presented in this study are available on request from the first author.

Acknowledgments

We would like to express our deepest gratitude to the Hawassa University Institute of Technology for their support in conducting this research. We thank the global Earth System Grid Federation for providing the CORDEX data. We would also like to thank the RCM data source website: https://esgf-node.llnl.gov/projects/esgf-llnl/ and the National Meteorological Service Agency of Ethiopia for providing the observed station data.

References

1. Adenuga, K. I., Mahmoud, A. S., Dodo, Y. A., Albert, M., Kori, S. A., & Danlami, N. J. (2021). Climate change adaptation and mitigation in sub-saharan African countries. Energy and Environmental Security in Developing Countries, 393–409.
2. Agha, O., Bağçacı, S. Ç., & Şarlak, N. (2017). Homogeneity analysis of precipitation series in North Iraq. IOSR Journal of Applied Geology and Geophysics, 5(03), 57–63.
3. Akinsanola, A. A., Ogunjobi, K. O., Gbode, I. E., & Ajayi, V. O. (2015). Assessing the Capabilities of Three Regional Climate Models over CORDEX Africa in Simulating West African Summer Monsoon Precipitation. Advances in Meteorology, 2015, e935431. https://doi.org/10.1155/2015/935431

4. Anose, F. A., Beketie, K. T., Zeleke, T. T., Ayal, D. Y., Feyisa, G. L., & Haile, B. T. (2022). Spatiotemporal analysis of droughts characteristics and drivers in the Omo-Gibe River basin, Ethiopia. Environmental Systems Research, 11(1), 3. https://doi.org/10.1186/s40068-022-00246-8
5. Asfaw, A., Bantider, A., Simane, B., & Hassen, A. (2021). Smallholder farmers' livelihood vulnerability to climate change-induced hazards: Agroecology-based comparative analysis in Northcentral Ethiopia (Woleka Sub-basin). Heliyon, 7(4), e06761.
6. Asseng, S., Ewert, F., Martre, P., Rötter, R. P., Lobell, D. B., Cammarano, D., Kimball, B. A., Ottman, M. J., Wall, G. W., & White, J. W. (2015). Rising temperatures reduce global wheat production. Nature Climate Change, 5(2), 143–147.
7. Ayugi, B., Nadoya, H. N., Babaousmail, H., Karim, R., Iyakaremye, V., Lim Kam Sian, K., & Ongoma, V. (2021). Evaluation and projection of mean surface temperature using CMIP6 models over East Africa. Journal of African Earth Sciences. https://doi.org/10.1016/j.jafrearsci.2021.104226
8. Bayissa, Y., Tadesse, T., Demisse, G., & Shiferaw, A. (2017). Evaluation of satellite-based rainfall estimates and application to monitor meteorological drought for the Upper Blue Nile Basin, Ethiopia. Remote Sensing, 9(7), 669.
9. Caya, D., Laprise, R., Giguère, M., Bergeron, G., Blanchet, J. P., Stocks, B. J., Boer, G. J., & McFarlane, N. A. (1995). Description of the Canadian regional climate model. Water, Air, and Soil Pollution, 82(1), 477–482.
10. Demissie, T. A., & Sime, C. H. (2021a). Assessment of the performance of CORDEX regional climate models in simulating rainfall and air temperature over southwest Ethiopia. Heliyon, 7(8), e07791. https://doi.org/10.1016/j.heliyon.2021.e07791
11. Demissie, T. A., & Sime, C. H. (2021b). Assessment of the performance of CORDEX regional climate models in simulating rainfall and air temperature over southwest Ethiopia. Heliyon, 7(8), e07791. https://doi.org/10.1016/j.heliyon.2021.e07791
12. Dhidiou, A., Kamga, A., Klutse, N. A. B., Hewitson, B., Nikulin, G., & Lamptey, B. (2014). Climatology, annual cycle and interannual variability of precipitation and temperature in CORDEX simulations over West Africa. Int J Climatol, 34(7), 22412257.
13. Diaconescu, E. P., Gachon, P., Laprise, R., & Scinocca, J. F. (2016). Evaluation of precipitation indices over North America from various configurations of regional climate models. Atmosphere-Ocean, 54(4), 418–439.
14. Dibaba, W. T., Miegel, K., & Demissie, T. A. (2019). Evaluation of the CORDEX regional climate models performance in simulating climate conditions of two catchments in Upper Blue Nile Basin. Dynamics of Atmospheres and Oceans, 87, 101104.
15. Diro, G. T., Toniazzo, T., & Shaffrey, L. (2011). Ethiopian rainfall in climate models. In African climate and climate change (pp. 51–69). Springer.
16. Dosio, A., Panitz, H.-J., Schubert-Frisius, M., & Lüthi, D. (2015). Dynamical downscaling of CMIP5 global circulation models over CORDEX-Africa with COSMO-CLM: Evaluation over the present climate and analysis of the added value. Climate Dynamics, 44(9), 2637–2661.
17. Elzeiny, R., Khadr, M., Zahran, S., & Rashwan, E. (2019). Homogeneity analysis of rainfall series in the upper blue nile river basin, Ethiopia. Journal of Engineering Research, 3(September), 46–53.
18. Endris, H. S., Lennard, C., Hewitson, B., Dosio, A., Nikulin, G., & Panitz, H.-J. (2016). Teleconnection responses in multi-GCM driven CORDEX RCMs over Eastern Africa. Climate Dynamics, 46(9), 2821–2846. https://doi.org/10.1007/s00382-015-2734-7
19. Etana, D., van Wesenbeeck, C. F., & de Cock Buning, T. (2021). Socio-cultural aspects of farmers' perception of the risk of climate change and variability in Central Ethiopia. Climate and Development, 13(2), 139–151.
20. Francisco Ribeiro, P., & Camargo Rodriguez, A. V. (2020). Emerging advanced technologies to mitigate the impact of climate change in Africa. Plants, 9(3), 381.
21. Gadissa, T., Nyadawa, M., Behulu, F., & Mutua, B. (2018). The effect of climate change on loss of lake volume: Case of sedimentation in central rift valley basin, Ethiopia. Hydrology, 5(4), 67.
22. Gebrechorkos, S. H., Hülsmann, S., & Bernhofer, C. (2019). Changes in temperature and precipitation extremes in Ethiopia, Kenya, and Tanzania. International Journal of Climatology, 39(1), 18–30.
23. Giorgi, F., Jones, C., & Asrar, G. R. (2009). Addressing climate information needs at the regional level: The CORDEX framework. World Meteorological Organization (WMO) Bulletin, 58(3), 175.
24. Girma, R., Fürst, C., & Moges, A. (2022). Performance evaluation of CORDEX-Africa regional climate models in simulating climate variables over Ethiopian main rift valley: Evidence from Gidabo river basin for impact modeling studies. Dynamics of Atmospheres and Oceans, 99, 101317.
25. GUO, D.-L., SUN, J.-Q., & YU, E.-T. (2018). Evaluation of CORDEX regional climate models in simulating temperature and precipitation over the Tibetan Plateau. Atmospheric and Oceanic Science Letters, 11(3), 219–227. https://doi.org/10.1080/16742834.2018.1451725
26. Gutowski Jr, W. J., Giorgi, F., Timbal, B., Frigon, A., Jacob, D., Kang, H.-S., Raghavan, K., Lee, B., Lennard, C., & Nikulin, G. (2016). WCRP coordinated regional downscaling experiment (CORDEX): A diagnostic MIP for CMIP6. Geoscientific Model Development, 9(11), 4087–4095.
27. Hartkamp, A. D., De Beurs, K., Stein, A., & White, J. W. (1999). Interpolation techniques for climate variables, NRG-GIS series 99 – 01. CIMMyt, Mexico, DF.
28. Jacob, D., Bärring, L., Christensen, O. B., Christensen, J. H., de Castro, M., Déqué, M., Giorgi, F., Hagemann, S., Hirschi, M., & Jones, R. (2007). An inter-comparison of regional climate models for Europe: Model performance in present-day climate. Climatic Change, 81(1), 31–52.
29. Luhunga, P., Botai, J., & Kahimba, F. (2016). Evaluation of the performance of CORDEX regional climate models in simulating present climate conditions of Tanzania. Journal of Southern Hemisphere Earth Systems Science, 66(1), 32–54. https://doi.org/10.1071/es16005
30. Ly, S., Charles, C., & Degre, A. (2011). Geostatistical interpolation of daily rainfall at catchment scale: The use of several variogram models in the Ourthe and Ambleve catchments, Belgium. Hydrology and Earth System Sciences, 15(7), 2259–2274.
31. Martynov, A., Laprise, R., Sushama, L., Winger, K., Šeparović, L., & Dugas, B. (2013). Reanalysis-driven climate simulation over CORDEX North America domain using the Canadian Regional Climate Model, version 5: Model performance evaluation. Climate Dynamics, 41(11), 2973–3005.

32. Mekonen, A. A., & Berlie, A. B. (2020). Spatiotemporal variability and trends of rainfall and temperature in the Northeastern Highlands of Ethiopia. Modeling Earth Systems and Environment, 6(1), 285–300.
33. Mendez, M., Maathuis, B., Hein-Griggs, D., & Alvarado-Gamboa, L.-F. (2020). Performance evaluation of bias correction methods for climate change monthly precipitation projections over Costa Rica. Water, 12(2), 482.
34. Moges, A. G. (2013). The challenges and policies of poverty reduction in Ethiopia. Ethiopian E-Journal for Research and Innovation Foresight (Ee-JRIF), 5(1).
35. Mueller, B., & Seneviratne, S. I. (2013). Hot days induced by precipitation deficits at the global scale. EGU General Assembly Conference Abstracts, EGU2013-11525.
36. Mutayoba, E., & Kashaigili, J. J. (2017). Evaluation for the performance of the CORDEX regional climate models in simulating rainfall characteristics over Mbarali River catchment in the Rufiji Basin, Tanzania.
37. Ofoegbu, C., Chirwa, P. W., Francis, J., & Babalola, F. D. (2019). Assessing local-level forest use and management capacity as a climate-change adaptation strategy in Vhembe district of South Africa. Climate and Development, 11(6), 501–512.
38. Ongoma, V., Chen, H., & Gao, C. (2019). Evaluation of CMIP5 twentieth century rainfall simulation over the equatorial East Africa. Theoretical and Applied Climatology, 135(3), 893–910.
39. Pang, G., Wang, X., Chen, D., Yang, M., & Liu, L. (2021). Evaluation of a climate simulation over the Yellow River Basin based on a regional climate model (REMO) within the CORDEX. Atmospheric Research, 254, 105522.
40. Platonov, V., & Kislov, A. (2020). High-Resolution COSMO-CLM Modeling and an Assessment of Mesoscale Features Caused by Coastal Parameters at Near-Shore Arctic Zones (Kara Sea). Atmosphere, 11(10), Article 10. https://doi.org/10.3390/atmos11101062
41. Samuelsson, P., Jones, C. G., Will\' En, U., Ullerstig, A., Gollvik, S., Hansson, U. L. F., Jansson, E., Kjellstro\" M, C., Nikulin, G., & Wyser, K. (2011). The Rossby Centre Regional Climate model RCA3: Model description and performance. Tellus A: Dynamic Meteorology and Oceanography, 63(1), 4–23.
42. Shiferaw, A., Tadesse, T., Rowe, C., & Oglesby, R. (2018). Precipitation extremes in dynamically downscaled climate scenarios over the Greater Horn of Africa. Atmosphere, 9(3), 112.
43. Stefanidis, S., Dafis, S., & Stathis, D. (2020). Evaluation of regional climate models (RCMs) performance in simulating seasonal precipitation over Mountainous Central Pindus (Greece). Water, 12(10), 2750.
44. Taylor, K. E., Stouffer, R. J., & Meehl, G. A. (2012). An overview of CMIP5 and the experiment design. Bulletin of the American Meteorological Society, 93(4), 485–498.
45. Teshome, A., & Zhang, J. (2019). Increase of extreme drought over Ethiopia under climate warming. Advances in Meteorology, 2019.
46. van Meijgaard, E., Van Ulft, L. H., Van de Berg, W. J., Bosveld, F. C., Van den Hurk, B., Lenderink, G., & Siebesma, A. P. (2008). The KNMI regional atmospheric climate model RACMO, version 2.1. KNMI De Bilt, The Netherlands.
47. Van Vooren, S., Van Schaeybroeck, B., Nyssen, J., Van Ginderachter, M., & Termonia, P. (2019). Evaluation of CORDEX rainfall in northwest Ethiopia: Sensitivity to the model representation of the orography. International Journal of Climatology, 39(5), 2569–2586.
48. Vidal, N. P., Manful, C. F., Pham, T. H., Stewart, P., Keough, D., & Thomas, R. (2020). The use of XLSTAT in conducting principal component analysis (PCA) when evaluating the relationships between sensory and quality attributes in grilled foods. MethodsX, 7, 100835.
49. Warnatzsch, E. A., & Reay, D. S. (2019). Temperature and precipitation change in Malawi: Evaluation of CORDEX-Africa climate simulations for climate change impact assessments and adaptation planning. Science of The Total Environment, 654, 378–392. https://doi.org/10.1016/j.scitotenv.2018.11.098
50. Welteji, D. (2018). A critical review of rural development policy of Ethiopia: Access, utilization and coverage. Agriculture & Food Security, 7(1), 55. https://doi.org/10.1186/s40066-018-0208-y
51. WMO. (2009). Guidelines on analysis of extremes in a changing climate in support of informed decisions for adaptation. World Meteorological Organization.
52. Worku, G., Teferi, E., Bantider, A., Dile, Y. T., & Taye, M. T. (2018). Evaluation of regional climate models performance in simulating rainfall climatology of Jemma sub-basin, Upper Blue Nile Basin, Ethiopia. Dynamics of Atmospheres and Oceans, 83, 53–63.
53. Yigezu Wendimu, G. (2021). The challenges and prospects of Ethiopian agriculture. Cogent Food & Agriculture, 7(1), 1923619. https://doi.org/10.1080/23311932.2021.1923619
54. Yimer, S. M., Bouanani, A., Kumar, N., Tischbein, B., & Borgemeister, C. (2022). Assessment of Climate Models Performance and Associated Uncertainties in Rainfall Projection from CORDEX over the Eastern Nile Basin, Ethiopia. Climate, 10(7), Article 7. https://doi.org/10.3390/cli10070095
55. Zadra, A., Caya, D., Côté, J., Dugas, B., Jones, C., Laprise, R., Winger, K., & Caron, L.-P. (2008). The next Canadian regional climate model. Phys Can, 64(2), 75–83.

Figures

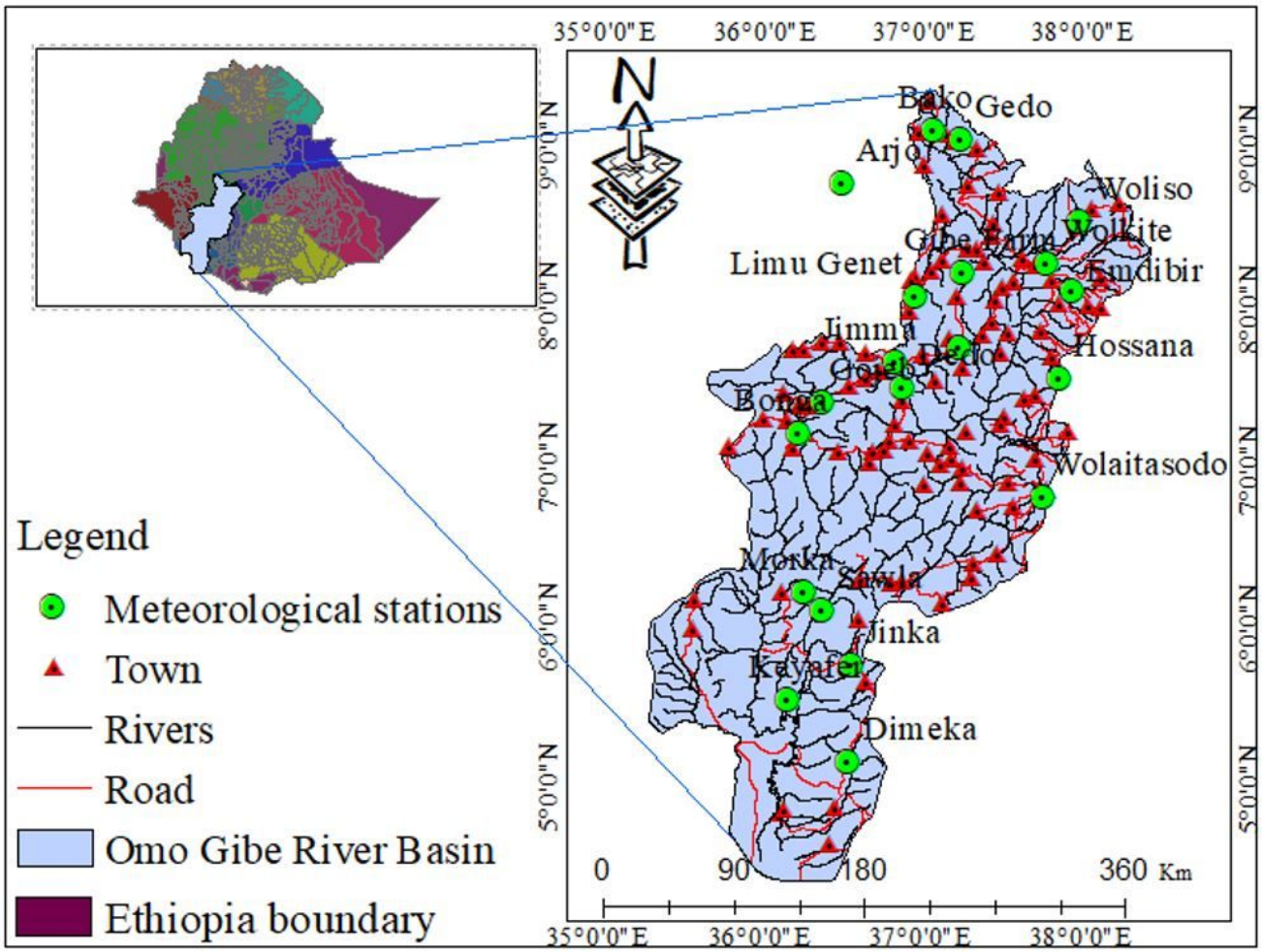

Figure 1

Map of the study area with the gauge stations of climate variables

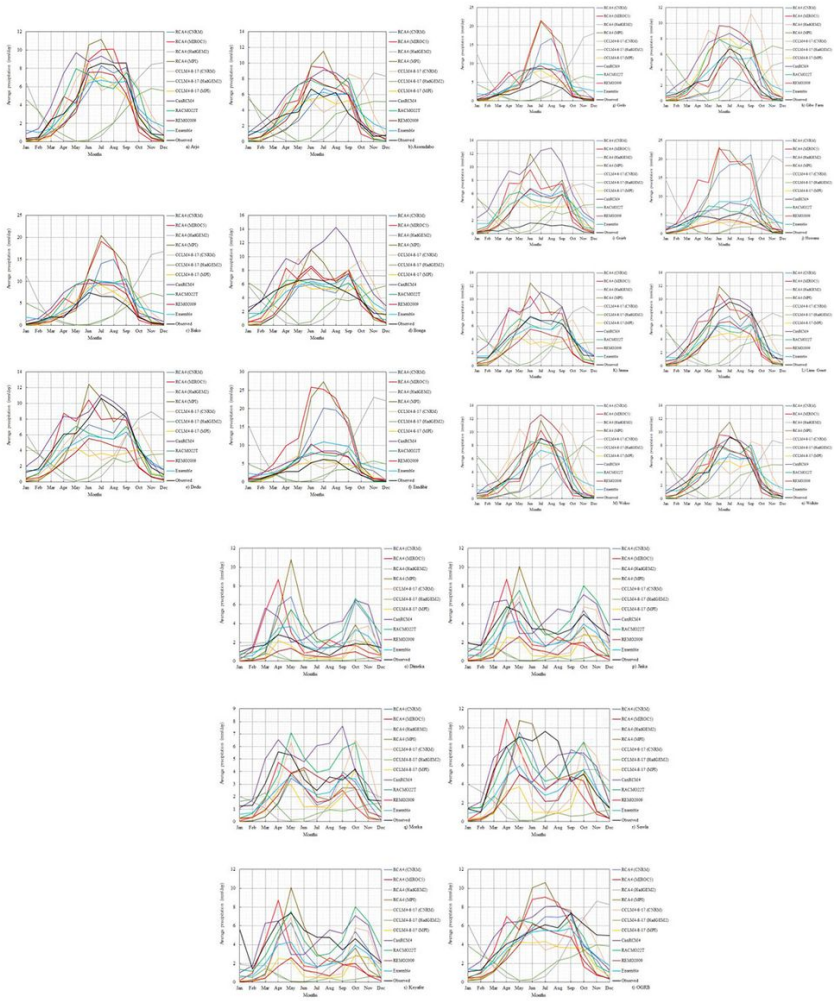

Figure 2

Mean monthly cycle of precipitation for the 10RCMs, multi-model ensemble (a-s), and observed for each station and across the entire OGRB(t).

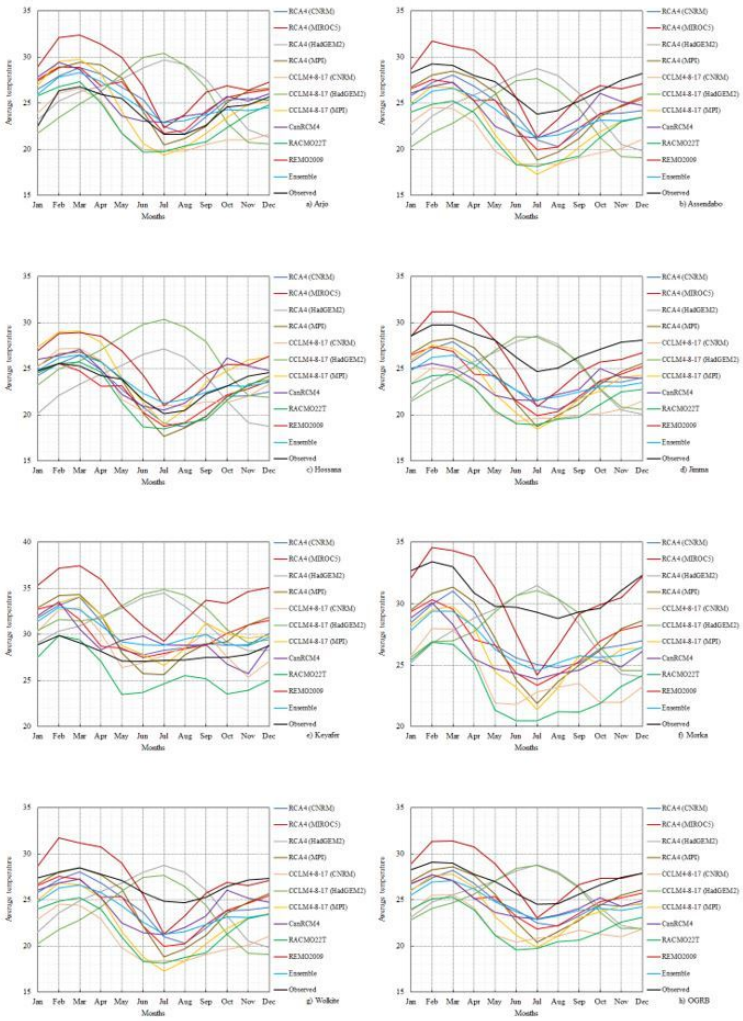

Figure 3

Mean monthly cycle of maximum air temperature for the 10RCMs, multi-model ensemble (a-g), and observed for the selected stations and across the entire OGRB (h).

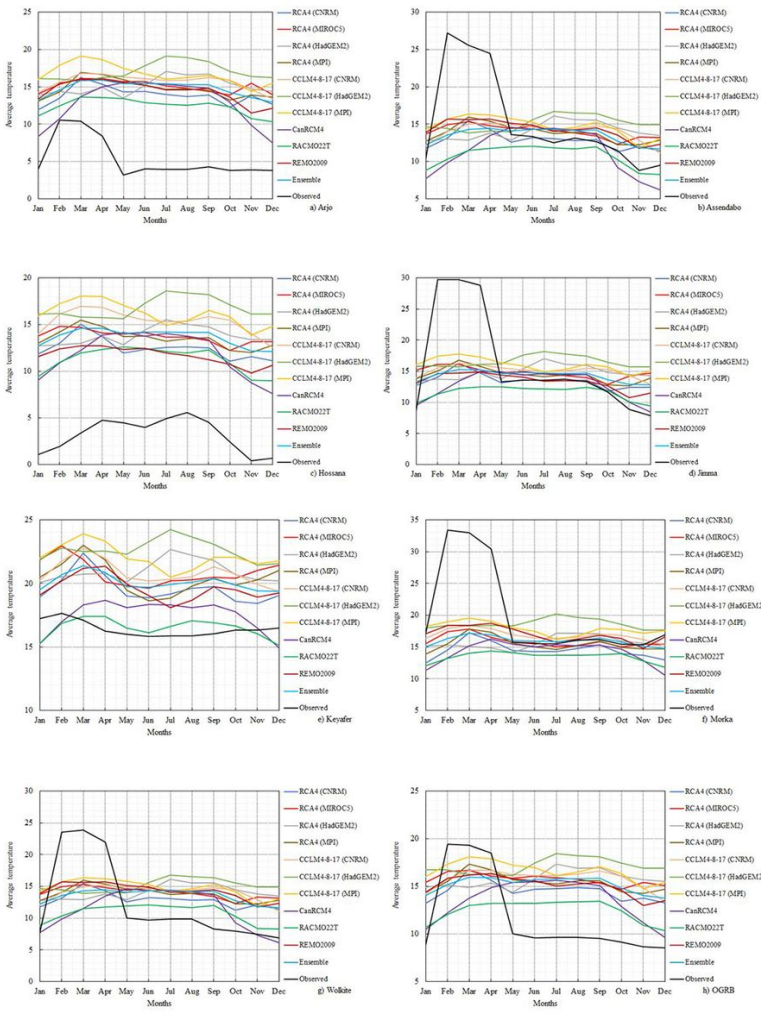

Figure 4

Mean monthly cycle of minimum air temperature for the 10RCMs, multi-model ensemble (a-g), and observed for the selected station and across the entire OGRB (h).

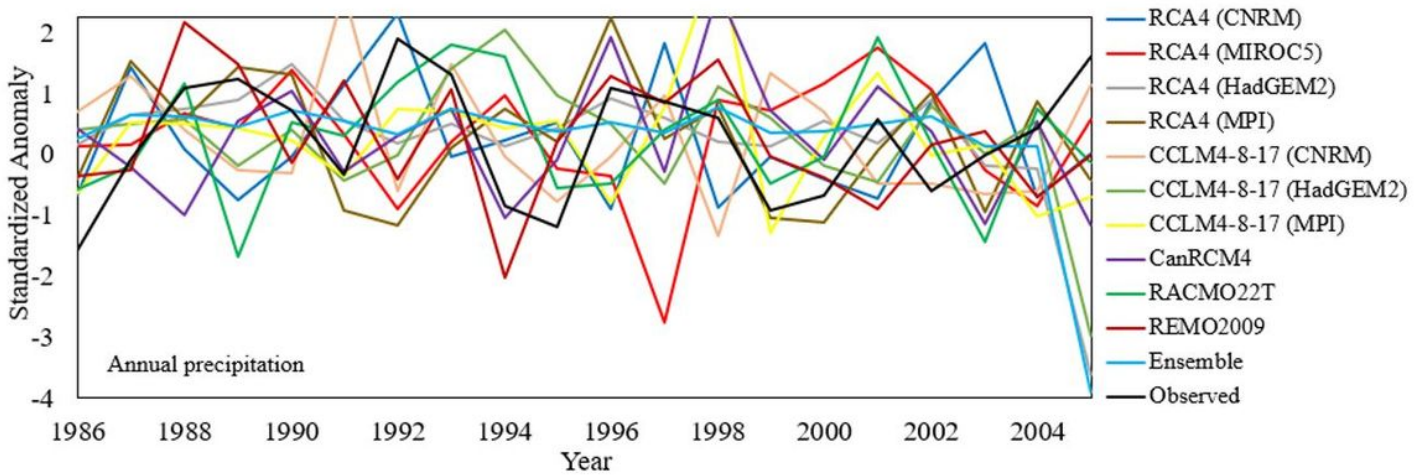

Figure 5

The interannual variability of the annual precipitation anomalies for the observed, the ten RCMs, and their ensemble mean.

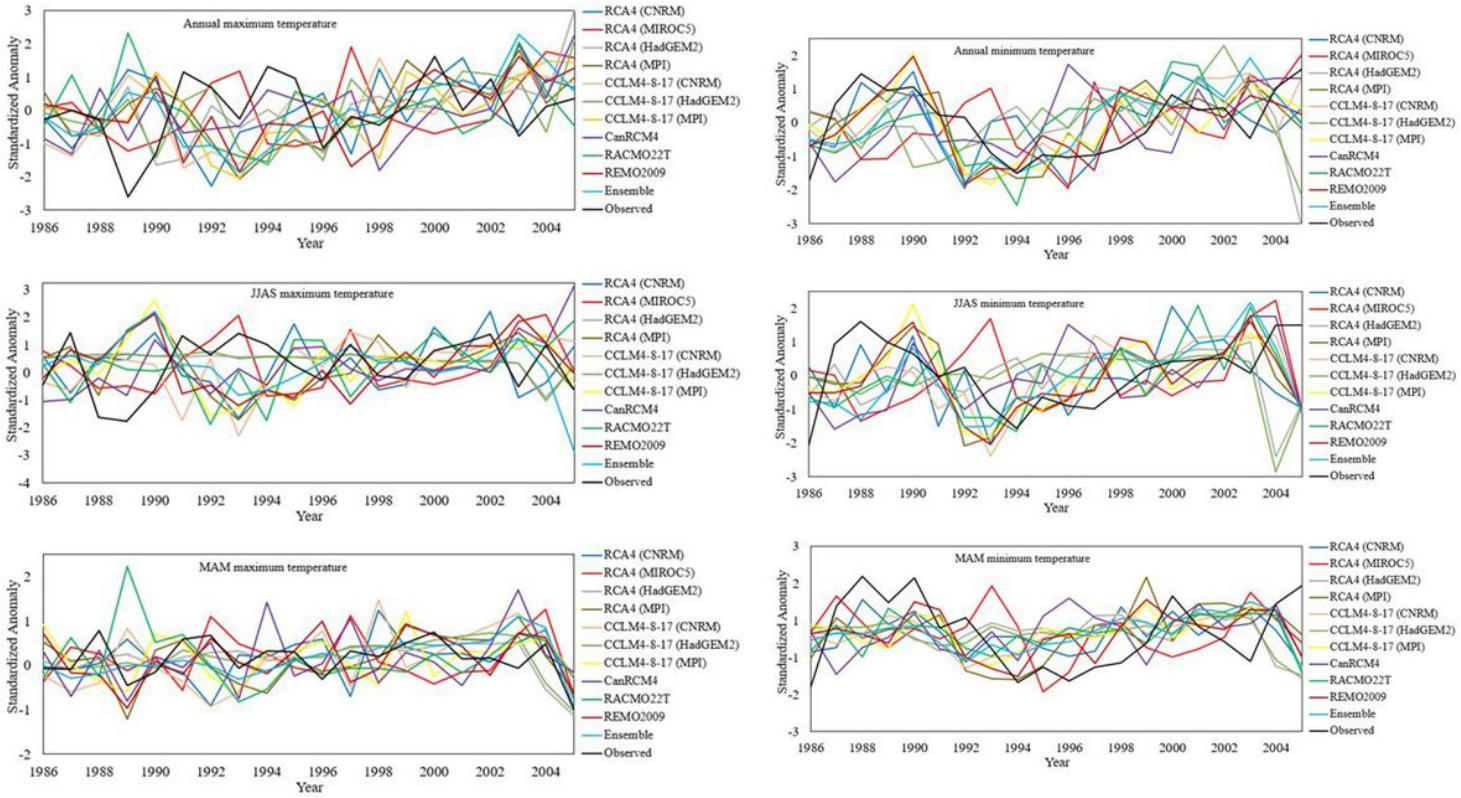

Figure 6

The interannual variability of seasonal minimum and maximum air temperature anomalies.

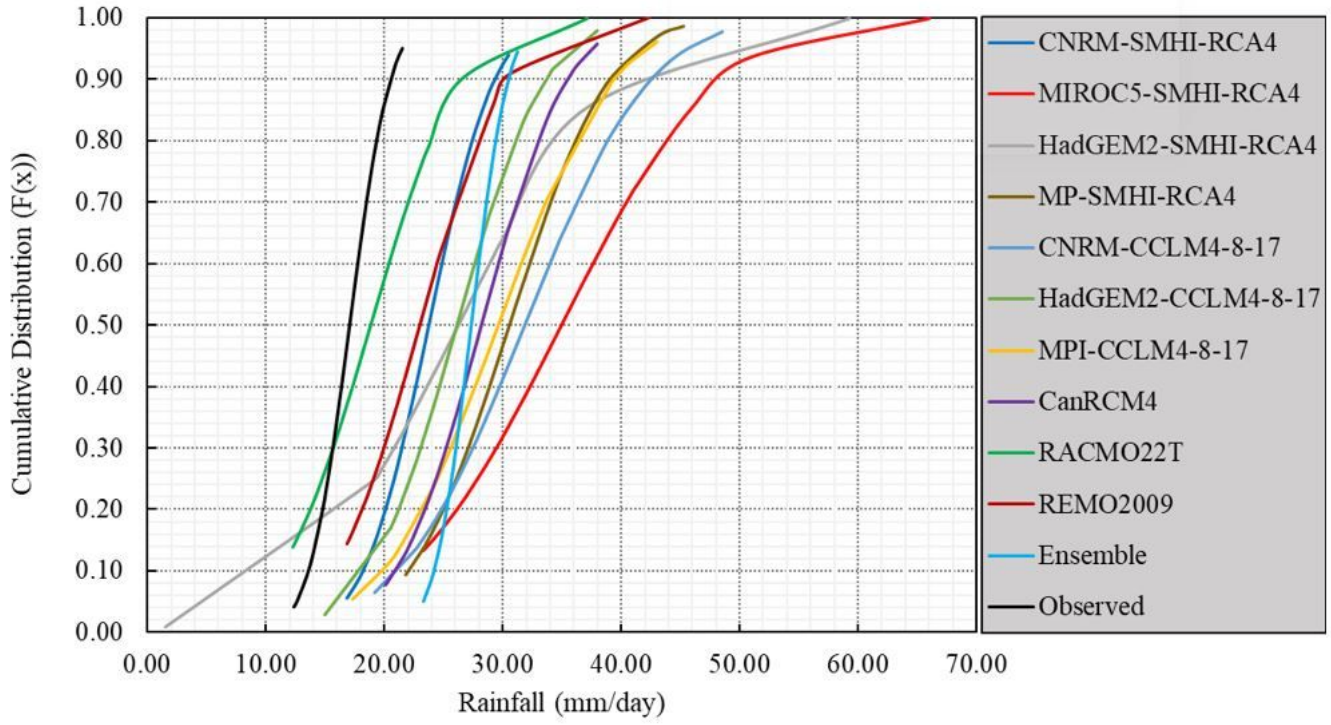

Figure 7

Cumulative distribution of areal rainfall over the entire OGRB

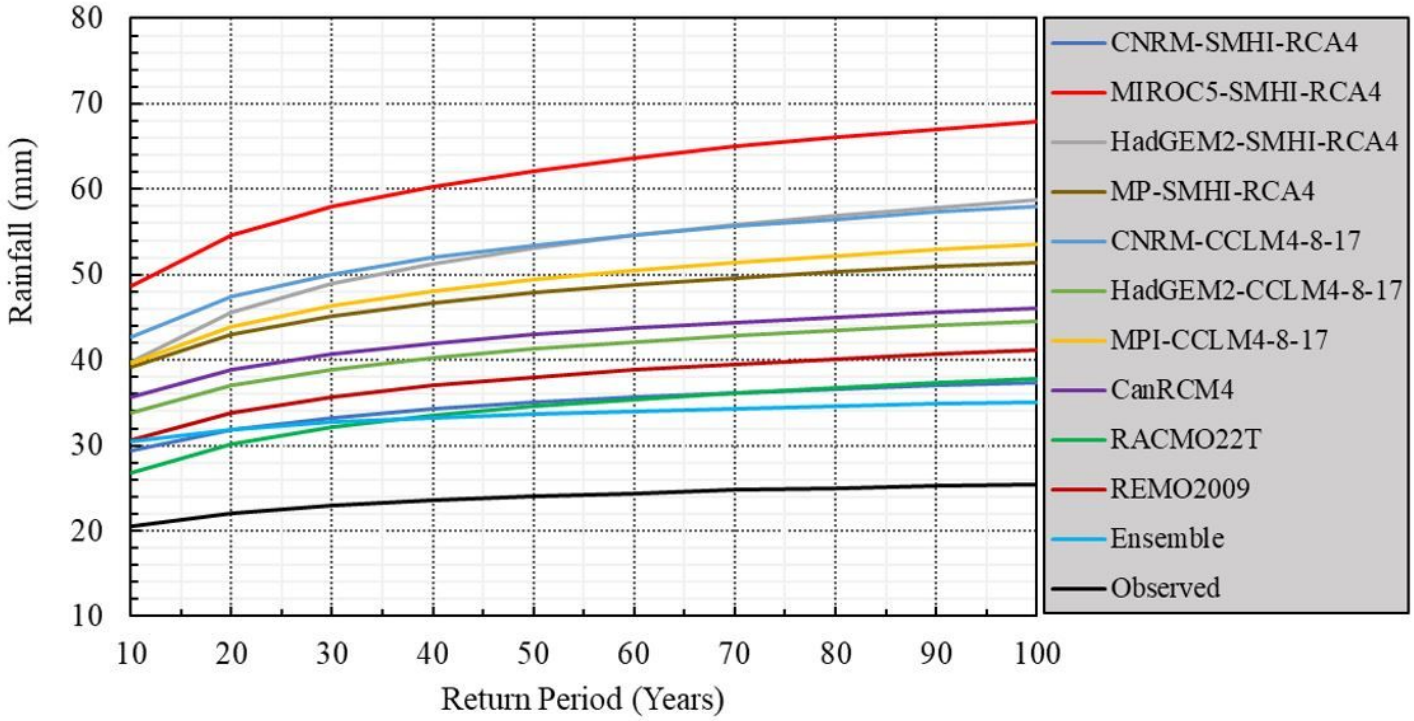

Figure 8

Annual extreme areal rainfall and return periods for RCMs and observed in the OGRB

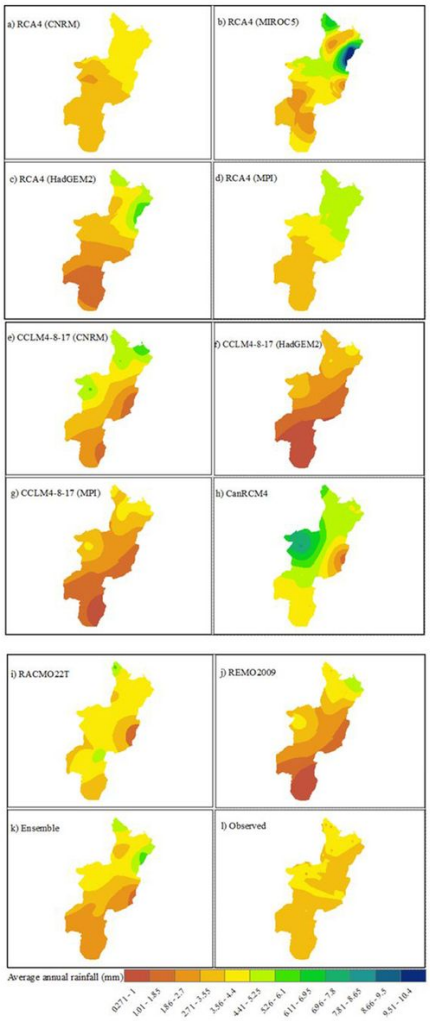

Figure 9

The spatial distribution of mean annual rainfall of ten RCMS and ensemble (a-k) and observed (i) from 1986 up to 2005 in the OGRB.